ANL/NE-12/4

The SAS4A/SASSYS-1 Safety Analysis Code System

Nuclear Engineering Division

ANL/NE-12/4

The SAS4A/SASSYS-1 Safety Analysis Code System

Chapter 4:
Reactor Point Kinetics, Decay Heat, and Reactivity Feedback

J. E. Cahalan, F. E. Dunn, J. P. Herzog, A. M White, and R. A. Wigeland
Nuclear Engineering Division
Argonne National Laboratory

January 31, 2012

TABLE OF CONTENTS

NOMENCLATURE

Symbol	Description	Units
A	Coefficient in EBR-II bowing reactivity.	\$
A_{cr}	Control rod driveline heat transfer area.	m^2
A_e	Nominal cross-sectional area of cladding.	m^2
A_f	Nominal cross-sectional area of fuel.	m^2
a	Above-core load pad elevation.	m
a_{cr}	Coefficient in control rod driveline reactivity feedback.	\$/m
B	Coefficient in EBR-II bowing reactivity.	\$
b_{cr}	Coefficient in control rod driveline reactivity feedback.	$\$/m^2$
C_{cr}	Control rod driveline specific heat.	J/kg-K
C_i	Delayed neutron precursor group i population.	
C_{rc}	Coefficient in simple radial core expansion reactivity feedback.	\$/K
D	Hex can flat-to-flat dimension.	m
D_z	Nominal axial node height in simple axial expansion reactivity feedback model.	m
E	Modulus of elasticity.	N/m^2
F_{cr}	Temperature multiplier in EBR-II control rod bank expansion model.	
F_{LowBU}	Fraction of fuel elements with burnup less than 2.9% in EBR-II.	
f_e	Cladding mesh height expansion factor.	
f_f	Fuel mesh height expansion factor.	
f_i	Channel flag in simple radial expansion reactivity model.	
H	Fuel height in EBR-II.	m
h_{cr}	Coolant to control rod driveline heat transfer coefficient.	W/m^2-k
h_{nk}	Normalized decay heat energy fraction for group n of curve k.	
I	Moment of inertia of beam cross-sectional area.	m^4
k	Reactor effective multiplication constant.	
δk	Reactivity, or change in the effective reactor multiplication constant.	
δk_{cl}	Cladding relocation reactivity.	
δk_{cr}	Control rod drive expansion reactivity.	

Symbol	Description	Units
δk_{cs}	Control system reactivity.	
δk_D	Fuel Doppler reactivity.	
δk_d	Fuel and cladding axial expansion reactivity.	
δk_{fu}	Fuel relocation reactivity.	
δk_{Na}	Coolant density or voiding reactivity.	
δk_p	User-programmed reactivity.	
δk_{re}	Core radial expansion reactivity.	
L	Elevation of top load pad.	m
L_{cr}	Control rod driveline length.	m
L_k	Reactor vessel wall length represented by compressible volume k or element k.	m
M	Bending moment.	N-m
M_{cr}	Control rod driveline mass.	kg
M_{GR}	Applied moment at grid plate.	N-m
M_1	Thermally induced bending moment in the core region.	N-m
M_2	Thermally induced bending moment above the core region.	N-m
m_{ij}	Fuel or cladding mass at node j in channel i in fuel and cladding relocation reactivity.	kg
N	Fuel, sodium, or steel atom density in EBR-II reactivity model.	atm/m^3
N_c	Number of channels.	
N_s	Number of subassemblies per channel.	
P	Radial force at the above core load pad.	N
P_i	Normalized power in interval i of irradiation history for decay heat precursor initial condition.	
Q	Space and time dependent nodal power.	W
R_e	Cladding nodal reactivity worth in simple axial expansion reactivity model.	kg^{-1}
R_f	Fuel nodal reactivity worth in simple axial expansion reactivity model.	kg^{-1}
R_i	Radial fuel reactivity worth shape factor in EBR-II reactivity model.	
R_1	Minimum core radius at above-core load pad in detailed radial expansion model.	m
R_2	Minimum core radius at top load pad in detailed radial expansion model.	m

Symbol	Description	Units
R_3	Maximum core radius at restraint ring in detailed radial expansion.	m
$\vec{r}$	Reactor spatial position vector.	
S	Space-dependent steady-state nodal power.	W
S_{GR}	Subassembly slope with respect to vertical at the grid plate.	m/m
S_{GRMAX}	Maximum subassembly slope with respect to vertical at the grid plate.	m/m
T	Temperature.	K
$\bar{T}$	Average temperature.	K
ΔT	Hexcan flat-to-flat temperature difference.	K
T_{by}	Bypass region temperature.	K
T_{ch}	Reflector steel temperature.	K
T_{cr}	Control rod driveline temperature.	K
T_{cv1}	Inlet plenum coolant temperature.	K
T_{cv2}	Outlet plenum coolant temperature.	K
T_e	Cladding temperature.	K
T_f	Fuel temperature.	K
$\bar{T}_f$	Average fuel temperature.	K
ΔT_f	Fuel temperature change.	K
$\Delta \bar{T}_{favg}$	Average fuel temperature change.	K
$\bar{T}_{floc}$	Average fuel temperature for a channel.	K
T_i	Plenum coolant temperature.	K
T_{in}	Coolant inlet temperature.	K
ΔT_{in}	Coolant inlet temperature change.	K
T_j	Reflector coolant temperature.	K
$\bar{T}_k$	Average vessel wall temperature in k-th compressible volume or element.	K
$\bar{T}_{lr}$	Average coolant temperature in lower reflector.	K
T_{mm}	Mixed mean coolant core outlet temperature.	K
$\bar{T}_{\text{Na}}$	Average coolant temperature.	K
$\bar{T}_{rr}$	Average radial reflector coolant temperature.	K
T_{SLP}	Space and time dependent structure temperature.	K
$\bar{T}_{SLP}$	Space-average, time dependent structure temperature.	K
$\Delta \bar{T}_{SLP}$	Change in space-averaged structure temperature.	K

Symbol	Description	Units
ΔT_{ss}	Cladding temperature change.	K
$\bar{T}_{ss}$	Average cladding temperature.	K
T_{ui}	Coolant temperature in the upper internal structure region.	K
$\bar{T}_{ur}$	Average coolant temperature in the upper reflector.	K
t	Time.	s
Δt	Change in time.	s
V_{by}	Bypass region volume.	m^3
$V_c h$	Channel steel volume.	m^3
V_{cv1}	Inlet plenum volume.	m^3
V_{cv2}	Outlet plenum volume.	m^3
V_f	Fuel volume.	m^3
V_{GR}	Radial reaction at the grid plate.	
V_i	Plenum coolant volume.	m^3
V_i	Channel volume.	m^3
V_j	Reflector coolant volume.	m^3
V_k	Nodal volume at k in channel.	m^3
V_{Na}	Sodium volume in fuel/cladding gap.	m^3
V_{ss}	Cladding volume.	m^3
V_{ui}	Coolant volume in upper internal structure.	m^3
w_c	Core outlet flow rate.	kg/s
w_k	Core volume weighting for decay heat curve k.	
XAC	Distance from subassembly nozzle support to above core load pad.	m
XMC	Distance from subassembly nozzle support to core midplane.	m
x	Axial elevation in detailed radial core expansion model.	m
x_1	Elevation of lower axial blanket/lower reflector interface.	m
Y	Fraction of full power temperature rise.	
Y_e	Cladding Young's modulus.	
Y_f	Fuel Young's modulus.	
Y_{ss}	Cladding Young's modulus.	
y	Radial displacement with respect to the core radius at the grid plate.	m
Z_k	Axial fuel reactivity worth shape.	
Δz_{cr}	Control rod driveline expansion.	m

Symbol	Description	Units
z_0	Unexpanded axial mesh elevation.	m
Δz_n	Net control rod movement.	m
z_{ne}	Expanded cladding mesh elevation.	m
z_{nf}	Expanded fuel mesh elevation.	m
Δz_v	Reactor vessel expansion.	m
α	Subassembly hex can thermal expansion coefficient.	1/K
α_{cr}	Control rod driveline thermal expansion coefficients.	1/K
α_D	Local fuel Doppler coefficient.	
α_e	Cladding thermal expansion coefficient.	1/K
α_f	Fuel thermal expansion coefficient.	1/K
α_{jI}	Average coolant void fraction in axial node j of channel I.	
α_k	Reactor vessel thermal expansion coefficient.	1/K
α_{Lf}	Fuel thermal expansion coefficient.	1/K
α_{Lss}	Cladding thermal expansion coefficient.	1/K
$\alpha_{V\mathrm{Na}}$	Sodium volumetric thermal expansion coefficient.	1/K
β	Total effective delayed-neutron fraction	
β_{hnk}	Effective decay-heat group n power fraction for curve k.	
β_i	Effective delayed-neutron precursor group i fraction.	
δ_e	Cladding axial expansion.	m
δ_f	Fuel axial expansion.	m
ϵ_e	Claddding fractional thermal expansion.	
ϵ_{ex}	Effective axial expansion multiplier.	
ϵ_f	Fuel fractional thermal expansion.	
ζ	EBR-II reactivity parameter.	$
ζ_{bw}	EBR-II bowing reactivity parameter.	$
ζ_c	EBR-II coolant reactivity parameter.	$
ζ_{cr}	EBR-II control rod driveline reactivity parameter.	$
ζ_{fa}	EBR-II axial fuel expansion reactivity parameter.	$
ζ_{fr}	EBR-II radial fuel expansion reactivity parameter.	$
ζ_{lr}	EBR-II lower reflector reactivity parameter.	$
ζ_{rr}	EBR-II radial reflector reactivity parameter.	$
ζ_{ssa}	EBR-II axial cladding expansion reactivity parameter.	$
ζ_{ssr}	EBR-II radial cladding expansion reactivity parameter.	$

Symbol	Description	Units
ζ_{ur}	EBR-II upper reflector reactivity parameter.	\$
Λ	Prompt neutron lifetime.	s
λ_{hnk}	Decay heat group effective decay constant for group n for curve k.	1/s
λ_i	Delayed neutron precursor group i decay constant.	1/s
ρ_c	Local coolant void reactivity worth.	g^{-1}
$\Delta\rho_e$	Cladding axial expansion reactivity.	
$\Delta\rho_f$	Fuel axial expansion reactivity.	
ρ_u	Sodium density in outlet plenum.	kg/m^3
ϕ	Normalized fission power amplitude.	
ϕ_1	First order coefficient in normalized fission power amplitude expansion.	s^{-1}
ϕ_2	Second order coefficient in normalized fission power amplitude expansion.	s^{-2}
ψ_f	Normalized fission power.	
ψ_h	Normalized decay heat power.	
ψ_t	Normalized total power.	

REACTOR POINT KINETICS, DECAY HEAT, AND REACTIVITY FEEDBACK

4.1 Introduction

The purpose of the SAS4A/SASSYS-1 reactor point kinetics, decay heat, and reactivity feedback models is to provide an estimate of the reactor power level to be used in the prediction of energy deposition in the fuel. Reactor material temperature changes and relocations determine the reactivity, which in turn determines the reactor power level and the rate of heating of the reactor materials.

The SAS4A/SASSYS-1 reactor point kinetics, decay heat, and reactivity feedback models are based on concepts used in the SAS3A [4-1] computer code. A time-independent reactor power spatial shape is assumed, along with a space-independent (point) reactor kinetics model. The decay-heat model is taken intact from SAS3A, except that different channels can have different decay heat curves in SAS4A/SASSYS-1. First-order perturbation theory is used to predict reactivity feedback effects associated with material density changes. Fuel temperature (Doppler) effects are calculated assuming a logarithmic dependence on the local absolute temperature ratio, with a linearly dependent variation of the local Doppler coefficient on the coolant void fraction.

The fundamental basis for the assumptions of a time-independent power distribution, point kinetics, and first-order perturbation theory is the underlying supposition that the reactor neutron flux distribution is invariant in time. This means that in the transient simulation, the effects of changes in the reactor environment (geometry, dimensions, temperature and density distributions) on the neutron flux shape are neglected. This significantly reduces the complexity and computational expense of the overall neutronics model, with some loss of accuracy. In general, this inaccuracy can be expected to be significant mainly in the estimate of the reactivity feedback accompanying large-scale fuel material relocations, and large-scale fuel relocation is usually not included in a SAS4A/SASSYS-1 case.

The sections that follow describe the mathematical formulations for the total reactor power, delayed-neutron precursors, decay heat, and net reactivity. The numerical solution methods are described in Section 4.6, and subsequent sections provide details on code organization, data flow, input, and output.

4.2 Reactor Power

At any time t, the local power production at position $\vec{r}$ is assumed to be given by the space-time separated function:

$$Q(\vec{r}, t) = \psi_t(t) S(\vec{r}) \tag{4.2-1}$$

where $\psi_t(t)$ is the dimensionless, normalized power amplitude and $S(\vec{r})$ is the steady-state reactor power in watts being produced in an axial node at location $\vec{r}$. In terms of input quantities, $S(\vec{r})$ is given by the product of POW (Input Block 12, location 1) and PSHAPE (Input Block 62, location 6). Initially, the power amplitude has a value of unity and $S(\vec{r})$ is normalized to the total steady-state reactor power. Appendix 4.1 contains a

description of the internal normalization of PSHAPE performed by SAS4A/SASSYS-1. The time-dependent power amplitude is assumed to be made up of the sum of two components:

$$\psi_t(t) = \psi_f(t) + \psi_h(t) \tag{4.2-2}$$

where $\psi_h(t)$ comes from the decay of fission and capture products. These two components have been separated to allow the simulation of both short- and long-term transients.

The direct fission component of the power amplitude is given by

$$\psi_f(t) = \psi_f(0)\phi(t) \tag{4.2-3}$$

where $\phi(t)$ is the dimensionless, normalized fission power amplitude given by the point reactor kinetics model:

$$\dot{\phi}(t) = \phi(t)\frac{\delta k(t) - \beta}{\Lambda} + \sum_i \lambda_i C_i(t) \tag{4.2-4}$$

with the initial condition $\phi(0) = 1$.

In Eq. 4.2-4, $\delta k(t)$ is the net reactivity, β is the total effective delayed-neutron fraction, Λ is the effective prompt neutron generation time, and λ_i is the decay constant for the delayed-neutron precursor isotope whose normalized population is $C_i(t)$. The physical interpretation of the terms in the point reactor kinetics equation is made by Henry [4-2] and also by Bell and Glasstone [4-3].

4.3 Delayed-Neutron Precursors

The net rate of change of the delayed-neutron precursor population is given by

$$\dot{C}_i(t) = \beta_i \phi(t)/\Lambda - \lambda_i C_i(t) \tag{4.3-1}$$

where β_i is the effective delayed-neutron fraction for precursor i, and the initial, normalized steady precursor population is given by

$$C_i(0) = \beta_i/\lambda_i\Lambda \tag{4.3-2}$$

In terms of the individual precursor delayed-neutron fractions, the total effective delayed-neutron fraction is given as

$$\beta = \sum_i \beta_i \tag{4.3-3}$$

The number of delayed neutron precursors is entered in input variable NDELAY (Input Block 1, location 16), the effective delayed neutron fractions are entered in input array BETADN (Input Block 12, location 4), and the delayed neutron precursor decay constants are entered in input array DECCON (Input Block 12, location 10). The prompt neutron lifetime is entered in input variable GENTIM (Input Block 12, location 2).

4.4 Decay Heat

As mentioned above, different channels can have different decay heat characteristics. Up to five different sets of decay heat characteristics are allowed in the code, and the user specifies which set is used in each channel. Different sets of decay heat characteristics are required because driver assemblies, radial blanket assemblies, control rod assemblies, and radial reflector assemblies have different decay heat curves.

Define h_{nk} as the precursor concentration times energy release for decay heat in group n of decay heat curve k. Then it is assumed that

$$\frac{dh_{nk}}{dt} = \beta_{hnk}\phi(t) - \lambda_{hnk}h_{nk} \tag{4.4-1}$$

in the region using set k of characteristics, where

β_{hnk} = decay heat power fraction in group n of characteristic k,

λ_{hnk} = decay constant for group n of characteristic k,

and

ϕ = normalized fission power amplitude.

The solution to Eq. 4.4-1 for time zero is

$$h_{hk}(0) = \beta_{hnk}\int_{-\infty}^{0}\phi(t')e^{\lambda_{hnk}t'}dt' \tag{4.4-2}$$

The values of $\phi(t')$ for the irradiation history ($t' \le 0$) are determined from a user-supplied histogram that can be written as

$$\phi(t') = P_i \text{ for } t_i \le t' \le t_{i+1} \tag{4.4-3}$$

where P_i is a normalized reactor power level. The P_i are the various power levels of reactor operation prior to time zero, and the t_i are the times at which constants P_i change values. The input quantities are the constant power levels, a maximum of eight, normalized to unity at time zero, and the associated times of duration of each power level. The code then calculates the t_i from the times of duration.

Substituting Eq. 4.4-3 into Eq. 4.4-2 gives

$$h_{\hbar k}(0) = \frac{\beta_{\hbar nk}}{\lambda_{\hbar nk}} \sum_i P_i \left(e^{\lambda_{\hbar nk} t_{i+1}} - e^{\lambda_{\hbar nk} t_i} \right) \tag{4.4-4}$$

The initial fission-power fraction can then be calculated from

$$\psi_f(0) = 1 - \sum_k w_k \sum_n \lambda_{\hbar nk} h_{nk}(0) \tag{4.4-5}$$

where w_k is the internally-calculated fraction of the total power represented by set k.

The number of decay heat groups in each of the decay heat characteristic curves is specified as input variable NDKGRP (Input Block 1, location 17), and the number of decay heat characteristic curves is entered as NPOWDK (Input Block 1, location 45). The group power fractions are entered as BETADK (Input Block 12, location 260), and the group decay constants are entered as DKLAM (Input block 12, location 290). If desired, each characteristic decay curve may be renormalized to give a steady-state decay heat power fraction given by BETAHT (Input Block 12, location 320). The number of entries in the irradiation history power for each characteristic curve is given by NPDKST (Input block 12, location 46), and the tables of irradiation powers and times are entered as POWLVL (Input Block 12, location 325) and POWTIM (Input Block 12, location 365). If no irradiation power history is entered (NPDKST = 0), then an infinite irradiation at nominal power is assumed.

4.5 Net Reactivity

For applications other than EBR-II, the net reactivity in Eq. 4.2-5 is the sum of nine reactivity components:

$$\begin{aligned} \delta k(t) = {} & \delta k_p(t) + \delta k_{cs}(t) + \delta k_D(t) + \delta k_d(t) + \delta k_{\mathrm{Na}}(t) \\ & + \delta k_{re}(t) + \delta k_{cr}(t) + \delta k_{fu}(t) + \delta k_{cl}(t) \end{aligned} \tag{4.5-1}$$

where

δk_p = User-programmed reactivity,

δk_{cs} = Control system reactivity,

δk_D = Fuel Doppler feedback reactivity,

δk_d = Fuel and cladding axial expansion feedback reactivity,

δk_{Na} = Coolant density or voiding feedback reactivity,

δk_{re} = Core radial expansion feedback reactivity,

δk_{cr} = Control rod drive expansion feedback reactivity,

δk_{fu} = Fuel relocation reactivity feedback,

δk_{cl} = Cladding relocation reactivity feedback.

The reactivity feedback models available for these components are covered in the sections that follow. For EBR-II applications, the net reactivity is calculated as formulated in Section 4.5.9.

4.5.1 User-Programmed Reactivity

The user-programmed reactivity is specified by the user at execution time as either an input table or as subprogram FUNCTION PREA. It is intended to be used as a means of specifying any reactivity effect not explicitly modeled as a feedback. An example might be the simulation of a control rod withdrawal or insertion, or the dropping of a fuel subassembly during reloading.

The user-programmed reactivity option is triggered by setting IPOWER (Block 1, location 8) to 0. For NPREAT (Block 1, location 18) equal to 0, the value returned by the user-supplied subroutine function PREA is used as the programmed reactivity. For NPREAT > 0, NPREAT gives the number of pairs of values of programmed reactivity and time input on the standard input file in PREATB (Block 12, location 29) and PREATM (Block 12, location 49). A maximum of twenty pairs of programmed reactivity and time may be entered in PREATB and PREATM. These data are then either used directly or fit to curves according to the user's specification of input data IFIT (Block 1, location 95).

4.5.2 Control System Reactivity

The control system reactivity is the value supplied by the reactivity control signal (JTYPE = -1) generated by the control system model (see Chapter 6 and Input Block 5 - INCONT).

4.5.3 Fuel Doppler Feedback Reactivity

The fuel Doppler reactivity effect at any axial location in a subassembly is estimated from

$$T\frac{d(\delta k_D)}{dT_f} = \alpha_D \tag{4.5-2}$$

where T_f is the local, volume-averaged fuel temperature, and α_D is the local fuel Doppler coefficient, an input quantity. To obtain the Doppler reactivity feedback at time t, Eq. 4.5-2 is integrated from steady-state conditions to conditions at time t to obtain

$$\delta k_D(t) = \alpha_D \ln\left[T_f(t)/T_f(0)\right] \tag{4.5-3}$$

Eq. 4.5-3 is used at each axial location where a fuel temperature is calculated. The local fuel Doppler coefficient, α_D, is adjusted linearly between the input coolant-in (flooded) and coolant-out (voided) values to correct for the effect of coolant voiding on neutron leakage.

The coolant-in and coolant-out Doppler coefficients are entered as ADOP and BDOP (Input Block 62, locations 62 and 63), and the axial weighting of the Doppler coefficients is input as WDOPA (Input Block 62, location 64).

4.5.4 Fuel and Cladding Axial Expansion Feedback Reactivity

4.5.4.1 Simple Axial Expansion Reactivity Model

A simple model for the reactivity effects of thermal expansion of fuel and cladding is included in SAS4A/SASSYS-1. The simple thermal expansion feedback model is based on a few assumptions. It is assumed that before the start of the transient, a combination of fuel cracking, fuel re-structuring, and stress relaxation cause the gap between the fuel and the cladding to close, but there is little contact force between the fuel and the cladding. During the transient, if the cladding expands faster than the fuel, then the fuel-cladding gap opens, and the fuel can expand freely in the axial direction. If the fuel expands faster than the cladding, then the fuel binds with the cladding, and the axial expansion is determined by balancing the axial forces between the fuel and the cladding. Slip between fuel and cladding is ignored in this case.

For each axial node, j, in the core, the fuel and cladding expansion fractions are calculated as

$$\epsilon_f(j,t) = \alpha_f\left[T_f(j,t) - T_f(j,0)\right] \tag{4.5-4}$$

and

$$\epsilon_e(j,t) = \alpha_e[T_e(j,t) - T_e(j,0)] \tag{4.5-5}$$

where

α_f = fuel thermal expansion coefficient

α_e = cladding thermal expansion coefficient

T_f = average fuel temperature for axial node j

and

T_e = cladding mid-point temperature

If $\epsilon_e(j)$ is greater than $\epsilon_f(j)$, then the fuel axial expansion for node j is

$$\delta_f(j,t) = \epsilon_f(j,t) D_z(j) \tag{4.5-6}$$

and the cladding expansion is

$$\delta_e(j,t) = \epsilon_e(j,t) D_z(j) \tag{4.5-7}$$

where D_z is the nominal axial height of the node. If $\epsilon_f(j)$ is greater than or equal to $\epsilon_e(j)$, then a simple balance between the axial forces of the fuel and cladding gives

$$\delta_f(j,t) = \frac{\epsilon_f(j,t) Y_f A_f + \epsilon_e(j,t) Y_e A_e}{Y_f A_f + Y_e A_e} D_z(j) \tag{4.5-8}$$

and

$$\delta_e(j,t) = \delta_f(j,t) \tag{4.5-9}$$

where

Y_f = fuel Young's modulus

Y_e = cladding Young's modulus

A_f = nominal cross-sectional area of the fuel

and

A_e = nominal cross-sectional area of the cladding

The reactivity calculation is based on the fuel and cladding worth tables used by the code. First an unexpanded axial mesh, $z_0(j)$, is calculated using

$$z_0(1) = 0 \tag{4.5-10}$$

and

$$z_0(j+1) = z_0(j) + D_z(j) \tag{4.5-11}$$

Note that z_0 is zero at the bottom of the lower axial blanket.

New, expanded axial meshes for the fuel and cladding, $z_{nf}(j)$ and $z_{ne}(j)$, are calculated using

$$z_{nf}(1) = 0 \tag{4.5-12}$$

$$z_{ne}(1) = 0 \tag{4.5-13}$$

$$z_{nf}(j+1) = z_{nf}(j) + f_f(j) D_z(j) \tag{4.5-14}$$

and

$$z_{ne}(j+1) = z_{ne}(j) + f_e(j) D_z(j) \tag{4.5-15}$$

where

$$f_f(j) = 1 + \frac{\delta_f(j,t)}{D_z(j)} \tag{4.5-16}$$

and

$$f_e(j) = 1 + \frac{\delta_e(j,t)}{D_z(j)} \tag{4.5-17}$$

SAS4A/SASSYS-1 uses a fuel worth per unit mass, $R_f(j)$, and a cladding worth per unit mass, $R_e(j)$, defined on the original mesh, $z_0(j)$. If node j has been shifted and expanded so that

$$z_0(j) \le z_{nf}(j) \le z_0(j+1) \tag{4.5-18}$$

and

$$z_0(j+1) \le z_{nf}(j+1) \le z_0(j+2) \tag{4.5-19}$$

as in Figure 4.5-1, then $\Delta\rho_f(j)$, the fuel contribution to axial expansion feedback from node j is calculated as

$$\begin{aligned} \Delta\rho_f(j) = {} & m_f(j) R_f(j) \frac{z_0(j+1) - z_{nf}(j)}{z_{nf}(j+1) - z_{nf}(j)} \\ & + m_f(j) R_f(j+1) \frac{z_{nf}(j+1) - z_0(j+1)}{z_{nf}(j+1) - z_{nf}(j)} - m_f(j) R_f(j) \end{aligned} \tag{4.5-20}$$

A similar expression is used to calculate $\Delta\rho_e(j)$, the cladding contribution to axial expansion feedback. If $z_{nf}(j+1)$ has expanded past $z_0(j+2)$, then a summation over the appropriate nodes is used instead of Eq. 4.5-20.

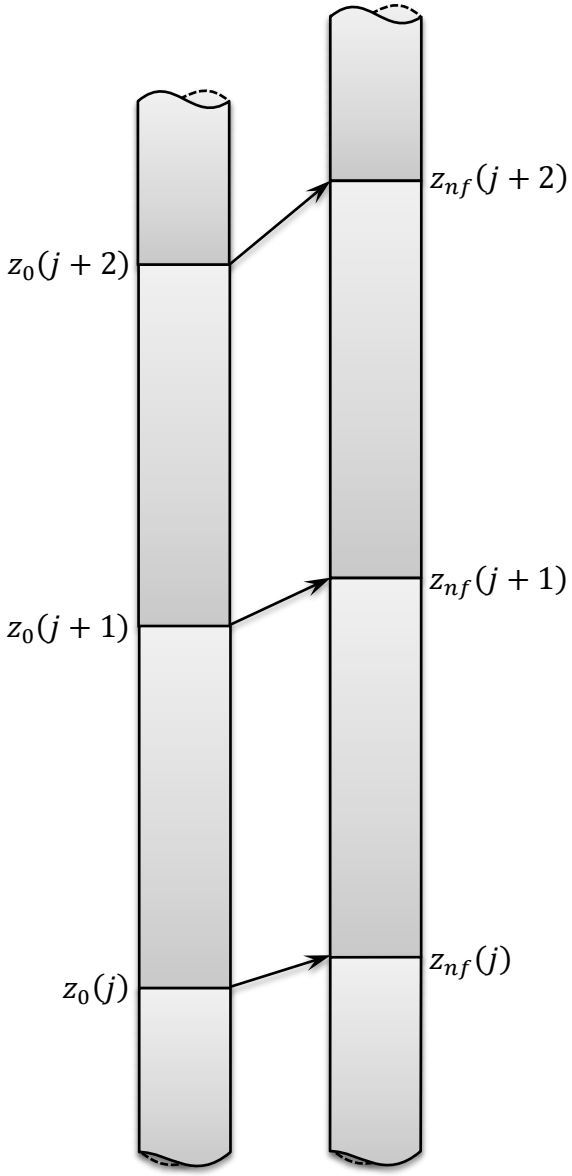

Figure 4.5-1. Original and Expanded Fuel Axial Meshes

The total reactivity change, δk_d, is

$$\delta k_d = \epsilon_{ex} \sum_j \left[\Delta\rho_f(j) + \Delta\rho_e(j)\right] \tag{4.5-21}$$

where ϵ_{ex} is an effective axial expansion multiplier.

The summation in Eq. (4.5-21) is only over the core nodes. The axial blankets are ignored in the fuel expansion feedback calculations. In order to obtain an accurate value for the axial expansion reactivity feedback, the fuel worth input for the upper axial blanket nodes must be the worth of core fuel in the blanket region.

The axial expansion feedback is calculated separately for each channel. An option has been added to the code to let the user specify the type of axial expansion desired with this model. In addition to the gap-dependent model described above, the user can choose free fuel expansion, cladding controlled expansion, or force balance controlled expansion at all times.

The cladding and fuel worth used in Eq. 4.5-20 are input in arrays CLADRA and FUELRA (Input Block 62, locations 160 and 208). The effective axial expansion multiplier in Eq. (4.5-21) is input as EXPCFF (Input Block 63, location 79). The simple axial expansion reactivity model is invoked by IAXEXP (Input Block 51, location 181).

4.5.4.2 DEFORM-4 Axial Expansion Reactivity Model

For any channel in which the DEFORM-4 module (see Chapter 8) has been specified, the axial expansion reactivity feedback will be calculated as described in Eqs. 4.5-10 through (4.5-21), but using fuel and cladding expanded axial mesh heights as calculated by DEFORM-4. The DEFORM-4 effective axial expansion multiplier is entered as EXPCOF (Input Block 13, location 1263).

4.5.5 Coolant Density Feedback Reactivity

Reactivity feedback effects from either single-phase coolant density changes or two-phase coolant boiling are calculated using the input coolant void reactivity worth table VOIDRA (Input Block 62, location 112). The reactivity feedback from coolant density and voiding changes is calculated from

$$\delta k_{\mathrm{Na}} = \sum_{I} \sum_{j} (\rho_c)_{jI} \alpha_{jI} \tag{4.5-22}$$

where

$(\rho_c)_{jI}$ = coolant void worth in axial segment j of channel I

and

α_{jI} = average coolant void fraction in segment j of channel I.

The local coolant void fraction is calculated based on either a) liquid coolant density changes from the initial steady-state condition, or b) combined liquid density and boiling-induced voiding density changes from the steady-state condition.

4.5.6 Radial Expansion Feedback Reactivity

4.5.6.1 Simple Radial Expansion Reactivity Model

Two radial expansion feedback models are available in SAS4A/SASSYS-1: a simple model described here and a more detailed model described in Section 4.5.6.2.

The simple radial expansion feedback model in SAS4A/SASSYS-1 is based on a model by Huebotter [4-4]. The radial growth of the core is determined by the expansion of the lower grid support structure and by the expansion of the duct walls at the above

core load pads. The expansion of the lower grid support structure is assumed to be proportional to the rise in the subassembly inlet temperature above its initial steady-state value. The expansion at the location of the above core load pads is assumed to be proportional to the change in the average structure temperature at this location.

The equations actually used in SAS4A/SASSYS-1 are

$$\delta k_{re} = C_{re}\left[\Delta T_{\text{in}} + \frac{\text{XMC}}{\text{XAC}}\left(\Delta \overline{T}_{SLP} - \Delta T_{\text{in}}\right)\right] \tag{4.5-23}$$

where

t = time, s

δk_{re} = reactivity change due to radial expansion, \$

C_{re} = radial expansion coefficient, \$/K

$\Delta T_{\text{in}} = T_{\text{in}}(t) - T_{\text{in}}(t_1)$, K

T_{in} = coolant inlet temperature, K

t_1 = time at the end of the first main time step, s

XMC = distance from nozzle support point to core midplane, m

XAC = distance from nozzle support point to above core load pad, m

$$\Delta \overline{T}_{SLP} = \overline{T}_{SLP}(t) - \overline{T}_{SLP}(\text{t}_1), \text{K} \tag{4.5-24}$$

$$\overline{T}_{SLP}(t) = \frac{\sum_i N_s(i) T_{SLP}(i,t) f_i}{\sum_i N_s(i) f_i} \tag{4.5-25}$$

$\overline{T}_{SLP}$ = average structure temperature at the above core load pads

$T_{SLP}(i,t)$ = structure temperature (outer structural radial node) in channel *i* at the axial node corresponding to the above core load pad

i = channel number

$N_s(i)$ = number of subassemblies represented by channel i

f_i = $\begin{cases} 1 \text{ if channel is to be included in the average} \\ 0 \text{ if channel is not to be included} \end{cases}$

An option has been included in the code to use the inlet plenum wall temperature instead of the coolant inlet temperature for T_{in}. This option can be used to account for

time delays in the heating of the lower grid support structure. Note that for coding simplicity the temperatures at the end of the first main time step are used as the reference values, rather than using steady-state temperatures for the reference. This makes very little difference in the results, since the changes in the inlet temperature and the outer structure node temperature above the core are normally extremely small during the first time step. Also, the user can choose which channels will be included in the averaging of Eq. 4.5-25 by specifying f_i for each channel (see Input Block 51, location 187, IRDEXP).

This model was not explicitly set up to account for subassembly bowing or flowering of the core, but the user can set arbitrary values for C_{re} and [XMC/XAC] in Eq. 4.5-23. Therefore, if the bowing reactivity effect is proportional to $\Delta\overline{T}_{\mathrm{SLP}}$ or to $\Delta\overline{T}_{\mathrm{SLP}} - \Delta\overline{T}_{\mathrm{in}}$, then bowing reactivity can be accounted for by adjusting C_{re} and XMC/XAC, which are entered as input variables RDEXPC and XMCXAC (Input Block 12, locations 78 and 79). The simple radial expansion model is invoked by specifying IRADEX (Input Block 1, location 36).

4.5.6.2 Detailed Radial Expansion Reactivity Model

The basic radial core expansion reactivity feedback model described in Section 4.5.6.1 incorporated several major assumptions that restricted the ability of the model to calculate the reactivity feedback accurately, particularly in extended transients. These assumptions include the following:

1. The reactivity feedback is determined solely by thermal expansions of the grid support plate and load pad region, with all regions having the same thermal expansion coefficient.
2. The displacement of the core midplane is sufficient to estimate the reactivity feedback from radial core expansion.
3. All of the subassembly load pads are in contact throughout the transients.

With these assumptions, the model does not explicitly account for subassembly bowing, and is not capable of calculating changes in core loading conditions during the course of a transient. This deficiency becomes especially important for the extended transients typically encountered for unprotected accidents.

In order to provide a more mechanistic approach to the calculation of the radial core expansion reactivity feedback, and to provide a framework for more detailed modeling as required, the following detailed model was developed. It is intended to overcome the restrictions associated with the assumptions listed above, and to allow a more appropriate use of results from detailed computer code simulations of core behavior, such as those obtained with NUBOW-3D [4-5].

4.5.6.2.1 Model Description

The approach taken in the development of the detailed model is to relate the reactivity feedback from radial core expansion to a change in the size of the core, in the same manner as a uniform dilation of the core is used to calculate the reactivity effect of a change in effective core radius. However, rather than maintain the cylindrical shape

associated with a uniform core dilation, an axial profile of core radius is calculated. During a transient, the changes in the axial profile are used in conjunction with a worth curve for radial core expansion to yield the reactivity feedback.

The axial profile of the core radius is obtained from the behavior of an average subassembly in the outer row of the core. The shape of this subassembly is determined by the relative location of the grid plate, the core, the load pads, and any core restraint rings. The shape is also affected by the thermal gradient across the subassembly, as this introduces additional bending of the subassembly. The subassembly is treated as a continuous beam subject to these conditions and restraints. The basic equation that describes these deflections is the differential equation of the elastic curve of the beam,

$$EI\frac{d^2y}{dx^2} = M_x \tag{4.5-26}$$

where

E = modulus of elasticity, N/m^2

I = moment of inertia of the beam cross-sectional area, m^4

M = bending moment, N-m

x = distance along the beam, m

y = distance perpendicular to the beam, m

This equation is solved subject to various loads and moments, depending on the state of the core. However, since only the displacement is needed, and the forces and moments are never evaluated, the solution is not dependent on the value of EI.

At present, the model is only applicable to the "limited free bow" type of restraint. For this type of restraint, there are load pads just above the top of the core (ACLP) and at the top of the subassembly (TLP). There is also a restraint ring (RR), or core former, around the core at the top load pad elevation. This restraint ring limits the outward motion of the top of the subassembly. With this type of restraint, the shape of the subassembly is determined by one of the following possibilities:

- Grid Plate/Subassembly Nozzle Clearances Not Exceeded
  - No contact at ACLP, RR or TLP

$$y(x) = \frac{M_1}{6EI(a - x_1)}(x - x_1)^3 \qquad \text{for } x_1 \le x \le a \tag{4.5-27a}$$

- No contact at ACLP; contact at RR

$$y(x) = \frac{M_1}{6EI(a - x_1)}(x - x_1)^3 + S_{GR}x \qquad \text{for } x_1 \le x \le a \qquad (4.5\text{-}27b)$$

$$S_{GR} = \frac{R_3 - \frac{M_1}{EI}\left[\frac{(a - x_1)(L - a)}{2} + \frac{(a - x_1)^2}{6}\right] - \frac{M_2}{EI}\frac{(L - a)^2}{2}}{L}$$

- No contact at ACLP; contact at TLP

$$y(x) = \frac{M_1}{6EI(a - x_1)}(x - x_1)^3 + S_{GR}x \qquad \text{for } x_1 \le x \le a \qquad (4.5\text{-}27c)$$

$$S_{GR} = \frac{R_2 - \frac{M_1}{EI}\left[\frac{(a - x_1)(L - a)}{2} + \frac{(a - x_1)^2}{6}\right] - \frac{M_2}{EI}\frac{(L - a)^2}{2}}{L}$$

- Contact at ACLP; no contact at TLP or RR

$$y(x) = \frac{M_1}{6EI(a - x_1)}(x - x_1)^3 + S_{GR}x \qquad \text{for } x_1 \le x \le a \qquad (4.5\text{-}27d)$$

$$S_{GR} = \frac{R_1 - \frac{M_1}{EI}\left[\frac{(a - x_1)^2}{6}\right]}{a}$$

- Contact at ACLP and RR

$$y(x) = \frac{M_1}{6EI(a - x_1)}(x - x_1)^3 - \frac{V_{GR}}{EI}\frac{x^3}{6} - \frac{C_1}{EI}x \qquad \text{for } x_1 \le x \le a \qquad (4.5\text{-}27e)$$

$$\frac{V_{GR}}{EI} = \frac{P}{EI}\left[1 - \frac{a}{L}\right]$$

$$\frac{P}{EI} = \frac{\frac{R_1 L}{a} - R_3 + \frac{M_1}{EI}\left(\frac{a^3}{3} - \frac{x_1 a^2}{2} + \frac{x_1^3}{6}\right)\frac{L/a - 1}{a - x_1} + \frac{M_2}{EI}\frac{(L - a)^2}{2}}{\frac{1}{3}\left(a^3 - \frac{x_1 a^2}{2} + \frac{x_1^3}{6}\right)}$$

$$\frac{C_1}{EI} = \frac{C_3}{EI} + \frac{M_1}{EI}\frac{x_1^2}{2(a - x_1)}$$

$$\frac{C_3}{EI} = -\frac{R_1}{a} + \frac{M_1}{EI}\frac{1}{a-x_1}\left[\frac{a^2}{6} - \frac{x_1 a}{2} + \frac{x_1^3}{6a}\right] - \frac{V_{GR}}{EI}\frac{a^2}{6}$$

- Grid plate/subassembly nozzle clearances exceeded
  - No contact at ACLP; contact at RR

$$y(x) = \frac{M_1}{6EI(a-x_1)}(x-x_1)^3 + S_{GRMAX}x - \frac{V_{GR}}{EI}\frac{x^3}{6} - \frac{M_{GR}}{EI}\frac{x^2}{2} \qquad \text{for } x_1 \le x \le a \qquad (4.5\text{-}27f)$$

$$\frac{M_{GR}}{EI} = -\frac{V_{GR}}{EI}L$$

  - No Contact at ACLP; contact at TLP

$$y(x) = \frac{M_1}{6EI(a-x_1)}(x-x_1)^3 + S_{GRMAX}x - \frac{V_{GR}}{EI}\frac{x^3}{6} - \frac{M_{GR}}{EI}\frac{x^2}{2} \qquad \text{for } x_1 \le x \le a \qquad (4.5\text{-}27g)$$

$$\frac{M_{GR}}{EI} = -\frac{V_{GR}}{EI}L$$

$$\frac{V_{GR}}{EI} = 3\frac{R_2}{L^3} - \frac{M_1}{EI}\left[\frac{3(a-x_1)(L-a)+(a-x_1)^2}{2L^3}\right] - \frac{M_2}{EI}\left[\frac{3(L-a)^2}{2L^3}\right] - 3\frac{S_{GRMAX}}{L^2}$$

  - Contact at ACLP; no contact at TLP or RR

$$y(x) = \frac{M_1}{6EI(a-x_1)}(x-x_1)^3 + S_{GRMAX}x - \frac{V_{GR}}{EI}\frac{x^3}{6} - \frac{M_{GR}}{EI}\frac{x^2}{2} \qquad \text{for } x_1 \le x \le a \qquad (4.5\text{-}27h)$$

$$\frac{M_{GR}}{EI} = -\frac{P}{EI}a$$

$$\frac{V_{GR}}{EI} = \frac{P}{EI}$$

$$\frac{P}{EI} = 3\frac{R_1}{a^3} - \frac{M_1}{EI}\frac{(a-x_1)^2}{2a^3} - 3\frac{S_{GRMAX}}{a^2}$$

- Contact at ACLP and RR

$$y(x) = \frac{M_1}{6EI(a-x_1)}(x-x_1)^3 + S_{GRMAX}x - \frac{V_{GR}}{EI}\frac{x^3}{6} - \frac{M_{GR}}{EI}\frac{x^2}{2} \qquad \text{for } x_1 \le x \le a \qquad (4.5\text{-}27\text{i})$$

$$\frac{M_{GR}}{EI} = -\frac{P}{EI}(L-a) - \frac{V_{GR}}{EI}L$$

$$\frac{V_{GR}}{EI} = \frac{P}{EI}\left[1 + \frac{a^3}{2L^3} - \frac{3a^2}{2L^2}\right] + \frac{3R_3}{L^3} - \frac{M_1}{EI}\left[3(a-x_1)(L-a) + (a-x_1)^2\right]/2L^3 - \frac{M_2}{EI}\left[3(L-a)^2\right]/2L^3 - 3S_{GRMAX}/L^2$$

$$\frac{P}{EI} = \left[R_3\left(\frac{3a^2}{L^2} - \frac{a^3}{L^3}\right)/2 - T_1 - \frac{M_1}{EI}\left[\left(\frac{3a^2}{L^2} - \frac{a^3}{L^3}\right)\frac{(L-a)}{4} + \left(\frac{a^2}{4L^2} - \frac{a^3}{12L^3} - \frac{1}{6}\right)(a-x)_1\right](a-x_1) - \frac{M_2}{EI}\left(\frac{3a^2}{L^2} - \frac{a^3}{L^3}\right)\frac{(L-a)^2}{4} + S_{GRMAX}\left(a + \frac{a^3}{L^2} - \frac{3a^2}{2L}\right)\right] / a^3\left(\frac{a^3}{12L^3} - \frac{a^2}{2L^2} + \frac{3a}{4L} - \frac{1}{3}\right)$$

- Contact at ACLP and TLP

$$y(x) = \frac{M_1}{6EI(a - x_1)}(x - x_1)^3 + S_{GRMAX}x - \frac{V_{GR}}{EI}\frac{x^3}{6} - \frac{M_{GR}}{EI}\frac{x^2}{2} \qquad \text{for } x_1 \le x \le a \qquad (4.5\text{-}27j)$$

$$\frac{M_{GR}}{EI} = \frac{P}{EI}(L-a) - \frac{V_{GR}}{EI}L$$

$$\frac{V_{GR}}{EI} = \frac{P}{EI}\left[1 + \frac{a^3}{2L^3} - \frac{3a^2}{2L^2}\right] + \frac{3R_2}{L^3} - \frac{M_1}{EI}\left[3(a-x_1)(L-a) + (a-x_1)^2\right]/2L^3 - \frac{M_2}{EI}\left[3(L-a)^2\right]/2L^3 - 3S_{GRMAX}/L^2$$

$$\frac{P}{EI} = \left[R_2\left(\frac{3a^2}{L^2} - \frac{a^3}{L^3}\right)/2 - R_1 - \frac{M_1}{EI}\left[\left(\frac{3a^2}{L^2} - \frac{a^3}{L^3}\right)\frac{(L-a)}{4} + \left(\frac{a^2}{4L^2} - \frac{a^3}{12L^3} - \frac{1}{6}\right)(a-x)_1\right](a-x_1) - \frac{M_2}{EI}\left(\frac{3a^2}{L^2} - \frac{a^3}{L^3}\right)\frac{(L-a)^2}{4} + S_{GRMAX}\left(a + \frac{a^3}{L^2} - \frac{3a^2}{2L}\right)\right] / a^3\left(\frac{a^3}{12L^3} - \frac{a^2}{2L^2} + \frac{3a}{4L} - \frac{1}{3}\right)$$

where

y = radial displacement with respect to the core radius at the grid plate

R_1 = minimum core radius at the above-core load pad with respect to the core radius at the grid plate

R_2 = minimum core radius at the top load pad with respect to the core radius at the grid plate

R_3 = maximum core radius at the restraint ring with respect to the core radius at the grid plate

x = axial elevation

x_1 = elevation of the lower axial blanket/lower reflector interface

a = elevation of the above core load pad

L = elevation of the top load pad

S_{GR} = subassembly slope with respect to vertical at the grid plate

S_{GRMAX} = maximum subassembly slope with respect to vertical at the grid plate

$\frac{M_1}{EI}$ = thermally induced bending moment in the core region

$\frac{M_2}{EI}$ = thermally induced bending moment in the above core region

V_{GR} = radial reaction at the grid plate

M_{GR} = applied moment at the grid plate

P = radial force at the above core load pad

EI = modulus of elasticity times the moment of inertia of the subassembly cross-sectional area

The use of the word contact in this context implies that either the outward motion is sufficient for the restraint ring to apply a force preventing further outward motion, or there is sufficient inward motion such that all of the intra-subassembly gaps in the load pad region(s) are eliminated, thus generating a force preventing further inward motion. A grid plate/subassembly nozzle clearance is required for the replacement of subassemblies, and results in a corresponding maximum possible deviation of the subassembly from vertical at the grid plate. When this clearance is exceeded, a moment is applied to the subassembly at the nozzle.

The subassembly is also subjected to a bending moment related to the temperature difference of opposite hex can walls within the subassembly. This temperature difference is converted into an equivalent bending moment, as described in the following section. The temperature difference increases linearly through the core region, from the lower axial blanket to the upper axial blanket. In the upper subassembly region, the temperature difference is assumed to be constant from the upper axial blanket to the top of the subassembly, with the value varying with time as the transient progresses.

The major assumptions incorporated in this model at present include the uniform distribution of core material in the radial direction at every axial elevation and the completely rigid subassembly load pads. Distributing the material uniformly at each axial elevation as the core radius changes is the same assumption used for the uniform core dilation calculation to obtain the radial core expansion reactivity feedback

coefficient, and implies that all of the subassemblies are moving in proportion to their distance from the center of the core. The radial expansion worth gradient and the intra-subassembly temperature gradients tend to be greatest at the edge of the active core, with the result that most of the reactivity feedback effect comes from movement of the outer row of subassemblies. Any movement in the central region of the core that is not proportional to the distance from the center of the core is expected to cause a minor effect. The accuracy of this assumption for any specific reactor core can be evaluated by comparison with results from NUBOW-3D [4-5].

The use of completely rigid subassembly load pads provides slightly greater expansion of the core during certain events as in an unprotected loss-of-flow, and less for other accidents, such as an unprotected loss-of-heat-sink transient. The error introduced by using this assumption is on the order of 15% to 20%, and can be design dependent. The incorporation of deformable load pads and "bridging" of subassemblies may be desirable, and is being considered for a future version of this model. The accuracy of this assumption can also be checked by comparison with NUBOW-3D.

Since the expression given by Eq. 4.5-26 is solved for the various core loading possibilities listed above, the resulting algebraic formulas are incorporated in the code. This avoids the need for a finite difference solution of Eq. 4.5-26, simplifying the computer coding and providing a rapid calculation of the core shape.

4.5.6.2.2 Code Description and Input Requirements

This section contains a description of the algorithm used for calculating the appropriate core shape. This calculation is performed at the start of the transient to establish the steady-state core configuration, and for every step during the transient. The use of the detailed radial core expansion reactivity feedback model requires some of the same input as the simple model plus several other variables. These will be discussed as their use occurs.

The optional model is activated by setting $|\text{IRADEX}| = 4$ or 5, (Blk. 1, Loc. 36), where a value of ±5 gives a much more detailed printout, while ±4 only gives results in the PSHORT printout. The first step is to calculate the average temperature of the above-core load pad (ACLP) and top load pad (TLP) regions. This is done using Eq. 4.5-25, as in the basic model. The model sets the location of the ACLP, so that JSTRDX (Blk. 51, Loc. 183) does not need to be input. The temperature of the grid plate can be given by either the inlet coolant temperature, or by the wall temperature of the compressible volume used to represent the inlet plenum in PRIMAR-4. This option is discussed in detail for the basic model, and is activated by setting IRADEX (Blk. 1, Loc. 36) to the appropriate negative value.

The next step is to calculate the equivalent core radius at the grid plate, the ACLP and the TLP. For this calculation, the following input is needed:

NSUBTC (Blk. 1, Loc. 51)	total number of subassemblies in the active core region, including internal blankets and control subassemblies
MTGRD (Blk. 1, Loc. 52)	material used for the grid plate
MTACLP (Blk. 1, Loc. 53) MTTLP (Blk. 1, Loc. 54)	ACLP and TLP, where 1 = 316 SS 2 = HT-9
PITCHG (Blk. 12, Loc. 409)	subassembly pitch at the grid plate at reference temperature TR (Blk. 13, Loc. 419).
PITCHA (Blk. 12, Loc. 410)	flat-to-flat dimension across the ACLP and TLP at reference temperature TR
PITCHT (Blk. 12, Loc. 411)	reference temperature TR.

Using the pitch at the grid plate along with the steady-state inlet temperature, the equivalent radius of the subassemblies in active core is calculated. As part of the calculation, there is a call to subroutine THRMEX that gives the material thermal expansion as a function of temperature for either 316 SS or HT-9. For the load pad regions, a minimum allowable core radius is calculated based on the size of the load pad region when all of the load pads are pushed together and there are no intra-subassembly gaps. This is possible since the model assumes the load pads all have the same temperature, as described above.

In addition to these dimensions, there are two other geometric constraints, as follows:

SLMAX (Blk. 12, Loc. 408)	maximum allowable slope of the subassembly at the grid plate with respect to vertical, based on subassembly nozzle/grid plate clearances and dimensions
TLPRRC (Blk. 12, Loc. 413)	clearance between the top load pads and the restraint ring

The value for SLMAX is calculated from the radial clearances of the subassembly nozzle/grid plate socket connection and the length of the connection. The maximum tilt of the subassembly occurs when the maximum radial motion of the nozzle is used, usually inward at the bottom of the nozzle and outward at the top. This number is design-dependent and can vary greatly, even when the subassembly sizes are comparable. The clearance between the top load pad region and the restraint ring is

determined by the maximum clearance that would occur between the subassemblies in the outer row of active core and the first row of radial blankets when all of the core subassembly load pads are pushed inward together and all of the radial blanket load pads are pushed outward against the restraint ring. The top load pad/restraint ring clearance is kept constant throughout the transient, i.e. the restraint ring expands as the top load pads expand thermally. This approximation tends to be conservative. Default values for these two input variables have been provided for cases where such detailed design information is not available. Design information should be used wherever possible, as the results can be especially sensitive to the value for SLMAX.

The only other input variable required for determining the core shape are those related to the thermally-induced bending moment:

BNDMM1 (Blk. 12, Loc. 414)	applied bending moment at the top of the core region, representing the flat-to-flat temperature difference in the radial direction for the subassemblies at the outer edge of the active core
BNDMM2 (Blk. 12, Loc. 415)	applied bending moment in the region above the core, representing the flat-to-flat temperature difference in the radial direction in this region for the subassemblies at the outer edge of active core.

The data on the temperature difference must be obtained from a code which performs detailed calculations of the steady-state subassembly temperatures with intersubassembly heat transfer, such as SUPERENERGY-2 [4-6]. Default values are included if such information is not available. The input variables can then be calculated using Eq. 4.5-28.

$$\text{BNDMM1} = \alpha \Delta T / D \tag{4.5-28}$$

where

α = mean thermal expansion coefficient of the subassembly hexcan, 1/K

ΔT = flat-to-flat temperature difference, K

D = hexcan flat-to-flat dimension, m

The model uses a linear variation in bending moment through the core region, from zero at the bottom of the core to BNDMM1 at the top. The bending moment BNDMM2 is applied uniformly from the top of the core to the top of the subassembly. In the transient, the bending moments are modified in proportion to the power-to-flow ratio changes.

Once all of these conditions have been calculated, the algorithm goes through a series of logic to determine the correct combination of forces and moments, as given above. The subassemblies are assumed to be vertical at the grid plate unless there are forces at the ACLP or TLP, or both, which would cause the subassembly to tilt. With the appropriate choice, the algebraic equation corresponding to that loading condition is evaluated for every axial node in the core region. In the printout, the algebraic equation selected is indicated by "CORE SHAPE MODEL =", where the value printed corresponds to the particular case as listed:

CORE SHAPE MODEL

	Steady-State	**Transient**
Grid plate/subassembly nozzle clearances not exceeded		
No contact at ACLP, RR or TLP	1.0	21.0
No contact at ACLP; contact at RR	2.0	22.0
No contact at ACLP; contact at TLP	3.0	23.0
Contact at ACLP; no contact at TLP or RR	4.0	24.0
Contact at ACLP and RR	5.0	25.0
Grid plate/subassembly nozzle clearances exceeded		
No contact at ACLP; contact at RR	8.0	28.0
No contact at ACLP; contact at TLP	9.0	29.0
Contact at ACLP; no contact at TLP or RR	10.0	30.0
Contact at ACLP and RR	11.0	31.0
Contact at ACLP and TLP	12.0	32.0

In the steady-state, the axial profile of core radius is stored for comparison during the transient. For each step during the transient, the process is repeated and the difference in core radius at each elevation is calculated.

The reactivity worth curve is based on the radial expansion coefficient for a uniform core dilation,

RDEXCF (Blk. 12, Loc. 412)	radial expansion coefficient for a uniform core dilation, $/m

This coefficient is then proportioned among the axial fuel nodes according to the axial power shape. The resulting worth curve provides the radial displacement worth for each axial node in the core. When used in combination with the deflections from steady-state described above, the reactivity feedback from each axial node is determined and the total reactivity feedback from radial core expansion is calculated by summing over the axial fuel nodes. As stated above, this is a very rapid calculation due to the use of

algebraic expressions for the subassembly shape, which are the solutions given in Eq. 4.5-27 for the various combinations of force and moments.

4.5.7 Control Rod Drive Expansion Feedback Reactivity

For the control rod drive feedback model, it is assumed that the control rod drives are washed by the outlet coolant from the core. Thermal expansion of the drives due to a rise in core outlet temperature will cause the control rods to be inserted further into the core, providing a negative reactivity component. On the other hand, if the control rod drives are supported on the vessel head, and if the core is supported by the vessel walls, then heating the vessel walls will either lower the core or raise the control rod drive supports, leading to a positive reactivity component. Both the control drive expansion and the vessel wall expansion are accounted for in SAS4A/SASSYS-1. This model is invoked with input variable ICREXP (Input Block 1, location 31).

A simple one-node treatment is used for calculating the temperature of the control rod drives. The equation used is

$$M_{cr}C_{cr}\frac{dT_{cr}}{dt} = h_{cr}A_{cr}(T_{ui} - T_{cr}) \tag{4.5-29}$$

where

M_{cr} = mass of the control rod drivelines, kg

C_{cr} = specific heat of the rod drivelines, J/kg-K

T_{cr} = control rod drive temperature, K

T_{ui} = coolant temperature in the upper internal structure region, K

h_{cr} = heat transfer coefficient between the coolant and the control rod drive, W/m^2-K

A_{cr} = heat transfer area between the coolant and the control rod drive, m^2

t = time, s

The product of the control rod driveline mass and specific heat is entered as input variable CRDMC (Input Block 12, location 75), and the product of the driveline heat transfer coefficient and area is entered as CRDHA (Input Block 12, location 76).

The coolant temperature in the upper internal structure region is calculated using

$$\frac{dT_{ui}}{dt} = w_c\frac{T_{mm} - T_{ui}}{\rho_u V_{ui}} \tag{4.5-30}$$

where

w_c = core outlet flow rate

T_{mm} = mixed mean coolant outlet temperature

ρ_u = sodium density in the outlet plenum

V_{ui} = coolant volume in the upper internal structure region

Initially both T_{ui} and T_{cr} are set equal to the steady-state mixed mean outlet temperature. The UIS volume, V_{ui} is entered as input variable UIVOL (Input Block 12, location 77).

During the transient calculation, Eq. 4.5-30 is approximated with

$$T_{ui}(t+\Delta t) = \frac{T_{ui}(t) + x\, T_{mm}(t+\Delta t)}{1+x} \tag{4.5-31}$$

where

$$x = \frac{w_c(t+\Delta t)\Delta t}{\rho_u V_{ui}} \tag{4.5-32}$$

For this calculation, only channels with positive outlet flow rates contribute to w_c and T_{mm}. Eq. 4.5-29 is approximated as

$$M_{cr}C_{cr}\frac{T_{cr}(t+\Delta t) - T_{cr}(t)}{\Delta t} = h_{cr}A_{cr}[T_{ui}(t+\Delta t) - T_{cr}(t+\Delta t)] \tag{4.5-33}$$

or

$$T_{cr}(t+\Delta t) = \frac{T_{cr}(t) + d\, T_{ui}(t+\Delta t)}{1+d} \tag{4.5-34}$$

where

$$d = \frac{h_{cr}A_{cr}}{M_{cr}C_{cr}}\Delta t \tag{4.5-35}$$

The axial expansion of the control rod drive, Δz_{cr}, is calculated as

$$\Delta z_{cr}(t) = L_{cr}\alpha_{cr}[T_{cr}(t) - T_{cr}(0)] \tag{4.5-36}$$

where L_{cr} is the length of the control rod drive washed by the outlet sodium, and α_{cr} is the thermal expansion coefficient. These data are entered as CRDLEN and CRDEXP (Input Block 12, locations 71 and 72).

The vessel wall expansion is calculated on the basis of the temperatures calculated by PRIMAR-4 for the walls of the liquid elements or compressible volumes that represent the vessel wall. For a typical pool reactor, the vessel wall would be the wall of the cold pool; but for some reactor designs a number of compressible volumes and liquid elements would be used to represent the vessel wall. The expansion of the vessel wall, Δz_v, is calculated as

$$\Delta z_v = \sum_k [\bar{T}_k(t) - \bar{T}_k(0)] L_k \alpha_k \tag{4.5-37}$$

where

$\bar{T}_k$ = average wall temperature of the k-th compressible volume or liquid element in the vessel wall

L_k = length of the vessel wall represented by the k-th compressible volume or element

α_k = thermal expansion coefficient of the vessel wall

The net movement, Δz_n, is calculated as

$$\Delta z_n = \Delta z_{cr} - \Delta z_v \tag{4.5-38}$$

and the reactivity feedback, δk_{cr}, is calculated as

$$\delta k_{cr} = a_{cr} \Delta z_n + b_{cr} (\Delta z_n)^2 \tag{4.5-39}$$

where a_{cr} and b_{cr} are user-supplied coefficients entered as ACRDEX and BCRDEX (Input Block 12, locations 73 and 74).

A multiple-node version of this model is in development, but has not been verified for production use.

4.5.8 Fuel and Cladding Relocation Feedback Reactivity

The fuel and cladding relocation reactivity feedbacks are calculated as the product of the input material reactivity worth (CLADRA and FUELRA, Input Block 62, locations 160 and 208) and the change in the axial material mass distribution since the initial steady-state condition. Symbolically this is represented by

$$\delta k(t) = \sum_i \sum_j \left(\frac{\Delta k}{\Delta m}\right)_{ij} \left[m_{ij}(t) - m_{ij}(0)\right]$$

where $(\Delta k/\Delta m)_{ij}$ is the material reactivity worth in axial node j of channel i, $m_{ij}(t)$ is the material mass at axial node j in channel i at time t, and $m_{ij}(0)$ is the initial steady-state node material mass. The input worth curves may be input on the fuel (MZ) mesh,

or the coolant (MZC) mesh according to the input valve of IREACZ (Input Block 51, location 365). The initial and transient axial mass distributions are computed internally from input design geometry and density data, and the fuel and cladding relocation models and solutions.

4.5.9 EBR-II Reactivity Feedback model

A reactor-specific set of reactivity feedback correlations has been implemented in SAS4A/SASSYS-1 for analysis of the EBR-II reactor and plant. The formulation of these correlations is based on the reactivity feedback model used in the NATDEMO computer program [4-7, 4-8], which is based on analysis of reactivity temperature coefficients in EBR-II Run 93 [4-9]. This documentation of the SAS4A/SASSYS-1 EBR-II reactivity feedback model is taken from notes provided by White [4-10] and Herzog [4-11].

In SAS4A/SASSYS-1, the EBR-II reactivity feedback is assumed to be composed of nine components. These components are: 1) fuel expansion, 2) coolant expansion, 3) stainless steel expansion, 4) axial reflector sodium expansion, 5) radial reflector sodium expansion, 6) fuel Doppler effect, 7) control rod bank expansion, 8) upper grid plate expansion, and 9) core subassembly bowing.

Each of these effects will be considered independently and the method in which the feedback magnitude is determined will be given. The source and nature (linear or nonlinear) of the term will also be discussed.

The reactivity in a steady state critical reactor is defined as zero. In the EBR-II feedback calculation, a parameter, which shall be named $\zeta(0)$, is defined at time zero (this treatment is not used in the other reactivity calculations performed by SASSYS). At later times, $\zeta(t)$ is calculated. The difference, $\delta k(t) = \zeta(t) - \zeta(0)$, is the reactivity introduced from feedback effects at time *t*.

4.5.9.1 Fuel Expansion

Both radial and axial expansion of the fuel are considered to be linear terms.

4.5.9.1.1 Axial Expansion

The method used is derived from Ref. 4-12. It has been modified to include the possibility that contact can occur between the fuel and cladding, thus altering the expression for the amount of expansion. Correlations from the Metallic Fuels Handbook [4-13] are used to evaluate the linear expansion coefficient and Young's modulus for the fuel and cladding types used in EBR-II fuel elements. First, the following correlation is used to determine the coefficient of linear expansion for U-5FS fuel:

$$\alpha_{LF} = \begin{cases} 1.264\times10^{-5} - 1.7964\times10^{-9}\bar{T} + 2.0532\times10^{-11}\bar{T}^2 & \bar{T} < 941 \\ 1.73\times10^{-5} & 941 < \bar{T} < 1048 \\ 1.775\times10^{-5} + 8.761\times10^{-9}\bar{T} - 3.717\times10^{-12}\bar{T}^2 & 1048 < \bar{T} < 1480 \\ 2.55\times10^{-5} & 1480 < \bar{T} \end{cases}$$

and for U-10Zr fuel, the following correlation is used:

$$\alpha_{LF} = \begin{cases} 1.658\times10^{-5} - 2.104\times10^{-8}\bar{T} + 3.345\times10^{-11}\bar{T}^2 & \bar{T} < 900 \\ 2.25\times10^{-5} & 900 < \bar{T} \end{cases}$$

and for U-10Zr-20Pu fuel, the following correlation is used:

$$\alpha_{LF} = \begin{cases} 1.73\times10^{-5} & \bar{T} < 868 \\ 1.98\times10^{-5} & 868 < \bar{T} \end{cases}$$

The $\overline{T}$ used here is the mass-average temperature for the fuel in a particular channel for a particular axial layer.

For SS316 or D-9 cladding, the steel linear thermal expansion coefficient is calculated from:

$$\alpha_{Lss} = 5.189\times10^{-5} - 6.4375\times10^{-4}\bar{T}^{-1/2} - 1.00862\times10^{-8}\bar{T}$$

and for HT-9 cladding the linear thermal expansion coefficient is calculated from:

$$\alpha_{Lss} = 1.62307\times10^{-6} + 2.84714\times10^{-8}\bar{T} - 1.65103\times10^{-11}\bar{T}^2$$

where $\bar{T}$ is the mass-average cladding temperature at a particular axial location in a particular channel.

Correlations [4-13] for the Young's modulus of metal fuels are functions of the fuel temperature and porosity P (Input Block 13, location 1073). The following correlation is used to determine the Young's modulus of U-5Fs fuel:

$$Y_f = \begin{cases} 1.5123\times10^{11}(1-1.2P)\left(1-1.06\dfrac{\bar{T}-588}{1405}\right) & \bar{T} < 923 \\ 1.5123\times10^{-11}(1-1.2P)\left(1-1.06\dfrac{\bar{T}-588}{1405}\right) - 0.3Y_f(923) & 923 < \bar{T} \end{cases}$$

For U-10Zr fuel, the following correlation is used:

$$Y_f = \begin{cases} 1.4349\times10^{11}(1-1.2P)\left(1-1.06\dfrac{\bar{T}-588}{1405}\right) & \bar{T} < 923 \\ 1.4349\times10^{-11}(1-1.2P)\left(1-1.06\dfrac{\bar{T}-588}{1405}\right) - 0.3Y_f(923) & 923 < \bar{T} \end{cases}$$

And for U-10Zr-20 Pu fuel, the following correlation is used:

$$Y_f = \begin{cases} 1.1149\times10^{11}(1-1.2P)\left(1-1.06\dfrac{\bar{T}-588}{1405}\right) & \bar{T} < 923 \\ 1.1149\times10^{-11}(1-1.2P)\left(1-1.06\dfrac{\bar{T}-588}{1405}\right) - 0.3Y_f(923) & 923 < \bar{T} \end{cases}$$

For SS316 or D-9 cladding, the steel Young's modulus is calculated from:

$$Y_{ss} = 2.01\times10^{11} - 7.929\times10^{7}\bar{T}$$

and for HT-9 cladding the Young's modulus is calculated from:

$$Y_{ss} = 2.137\times10^{11} - 1.0274\times10^{8}\bar{T}$$

The expression for the expansion in the fuel is

$$\delta_f = \alpha_{Lf}\Delta T_f$$

for no contact (fuel burnup < 2.9%), and

$$\delta_f = \frac{\alpha_{Lss}\Delta T_{ss}Y_{ss}A_{ss} + \alpha_{Lf}\Delta T_f Y_f A_f}{Y_{ss}A_{ss} + Y_f A_f}$$

for contact (fuel burnup > 2.9%), where α_{Lf} and α_{Lss} are the thermal expansion coefficients for the fuel and stainless steel, ΔT_f and ΔT_{ss} are the temperature changes for the fuel and stainless steel, Y_f and Y_{ss} are Young's modulus for the fuel and stainless steel, and A_f and A_{ss} are the cross sectional areas of the fuel and stainless steel.

As described above, the change in temperature is not calculated directly by the code. Instead, the code expands the expression into two terms: one involving steady state conditions, $\zeta(0)$, and the second involving the conditions at some time t, $\zeta(t)$. The reactivity feedback is determined using the expression $\delta k(t) = \zeta(t) - \zeta(0)$. The parameter ζ due to the expansion can be expressed as:

$$\zeta_{fa} = -\left[\left(\frac{\partial k}{\partial N/N}\right)_f - \left(\frac{\partial k}{\partial H/H}\right)_f\right]\frac{\alpha_{Lss}\bar{T}_{ss}Y_{ss}A_{ss} + \alpha_{Lf}\bar{T}_f Y_f A_f}{\left(Y_{ss}A_{ss} + Y_f A_f\right)\beta}$$

where β is the delayed neutron fraction, ζ_{fa} is the reactivity due to fuel axial expansion in dollars, $\left(\frac{\partial k}{\partial N/N}\right)_f$ is the change in k with a relative change in the number density of the fuel, and $\left(\frac{\partial k}{\partial H/H}\right)_f$ is the change in k with a relative change in the height of the fuel, for the case when the clad and fuel are in contact and

$$\zeta_{fa} = -\left[\left(\frac{\partial k}{\partial N/N}\right)_f - \left(\frac{\partial k}{\partial H/H}\right)_f\right]\frac{\alpha_{Lf}\bar{T}_f}{\beta}$$

for the case where there is no contact. The two partial derivatives in both of these expressions are entered as input to SAS4A/SASSYS-1 as input variables YKNF (Input Block 12, location 455) and YKHF (Input Block 12, location 456).

Because some channels will have both assemblies in which the cladding and fuel do contact and assemblies in which they do not contact, the code uses the equation:

$$\zeta_{fa} = -\left[\left(\frac{\partial k}{\partial N/N}\right)_f - \left(\frac{\partial k}{\partial H/H}\right)_f\right]\frac{\alpha_{Lss}\bar{T}_{ss}Y_{ss}A_{ss} + \alpha_{Lf}\bar{T}_f Y_f A_f}{(Y_{ss}A_{ss} + Y_f A_f)\beta}(1 - F_{\text{LowBU}})$$

$$-\left[\left(\frac{\partial k}{\partial N/N}\right)_f - \left(\frac{\partial k}{\partial H/H}\right)_f\right]\frac{\alpha_{Lf}\bar{T}_f}{\beta}F_{\text{LowBU}}$$

where F_{LowBU} is the fraction of pins with < 2.9% burnup. This fraction is entered to SAS4A/SASSYS-1 as variable FLOWBU (Input Block 62, location 267).

The temperature of the stainless steel (cladding) is determined using a weighted mass-average of the cladding temperature. The cladding is composed of three radial nodes. In the weighting, the middle node is given twice the weight of the two other nodes.

4.5.9.1.2 Radial Expansion

The radial expansion of the fuel contributes to the reactivity principally by displacing the bond gap sodium from the core. This displacement is of the sodium between the cladding and the fuel. Once the fuel reaches a burnup of 2.9% the cladding is in contact with the fuel and there is no additional displacement, and therefore, no additional reactivity change. The amount by which the fuel volume increases can be determined using a two dimensional isotropic approximation, i.e.: fuel volume increase is $V_f 2\alpha_{Lf}$. The fractional decrease in the sodium volume is then $V_f 2\alpha_{Lf}/V_{\text{Na}}$. The ζ value associated with this sodium expulsion is:

$$\zeta_{fr} = \left(-\frac{2V_f\alpha_{Lf}}{V_{\text{Na}}}\right)\left(\frac{\partial k}{\partial N/N}\right)_{\text{Na}}\frac{\bar{T}_f}{\beta}$$

when there is no contact and $\zeta_{fr} = 0$ when there is contact. In these expressions, $\left(\frac{\partial k}{\partial N/N}\right)_{\text{Na}}$ is the change in k with respect to a relative change in the number density of the sodium, which is entered as input variable YKNNA (Input Block 12, location 457). Therefore, the value of ζ for the radial expansion of the fuel can be expressed as:

$$\zeta_{fr} = \left(-\frac{2V_f\alpha_{Lf}}{V_{\text{Na}}}\right)\left(\frac{\partial k}{\partial N/N}\right)_{\text{Na}}\frac{\bar{T}_f}{\beta}F_{\text{LowBU}}$$

The same type of summation as given above is used to volume weight the reactivities (and temperatures, ζ values) from the different axial layers and channels.

4.5.9.2 Coolant Expansion

When the sodium coolant expands, it increases the leakage from the reactor, decreases sodium capture and results in spectral shifts. Sodium expansion is assumed to be a linear effect. The sodium coolant expansion is treated in a manner developed in Ref. 4.9. The equation used is:

$$\zeta_c = \left(\frac{\partial k}{\partial N/N}\right) \alpha_{V_{\mathrm{Na}}} \frac{\bar{T}_{\mathrm{Na}}}{\beta}$$

where $\alpha_{V_{\mathrm{Na}}}$ is the thermal volumetric expansion coefficient, $\bar{T}_{\mathrm{Na}}$ is the sodium temperature, and the sodium temperature is the value assigned by the code for a particular channel and axial layer. The sodium volumetric thermal expansion coefficient is calculated from the local sodium temperature in the correlation for the sodium volumetric thermal expansion coefficient given in Eq. 12.12-10.

The reactivity worths are summed in the manner described in the fuel axial expansion section. The sodium number density reactivity coefficient is entered as XKNNA (Input Block 12, location 457), the radial sodium reactivity worth factor is entered as XRNSHP (Input Block 62, location 269), and the axial sodium reactivity worth weighting is taken as the normalized axial shape of VOIDRA (Input Block 62, location 112).

4.5.9.3 Stainless Steel Expansion

Both axial and radial steel expansion coefficients are considered to be linear effects.

4.5.9.3.1 Axial Expansion

The axial expansion of the stainless steel cladding results in a decrease in the number density. The amount of expansion, as in the case of the fuel, is different for conditions where there is contact or no contact. In the event of no contact (burnup < 2.9%), the expression for the reactivity is:

$$\zeta_{ssa} = -\left(\frac{\partial k}{\partial N/N}\right)_{ss} \frac{\alpha_{Lss}\bar{T}_{ss}}{\beta}$$

where α_{Lss} is the linear thermal expansion coefficient for the cladding, and $\left(\frac{\partial k}{\partial N/N}\right)_{ss}$ is the change in k with respect to the relative number density in the stainless steel.

The partial derivative above is an input parameter, YKNSS (Input Block 12, location 458). If there is contact, the following expression applies:

$$\zeta_{ssa} = -\left(\frac{\partial k}{\partial N/N}\right)_{ss} \frac{\alpha_{Lss}\bar{T}_{ss}Y_{ss}A_{ss} + \alpha_{Lf}\bar{T}_f Y_f A_f}{\left(Y_{ss}A_{ss} + Y_f A_f\right)\beta}$$

The code therefore contains the expression:

$$\zeta_{ssa} = -\left(\frac{\partial k}{\partial N/N}\right)_{ss} \frac{\alpha_{Lss}\bar{T}_{ss}}{\beta} F_{\mathrm{LowBU}}$$

$$-\left(\frac{\partial k}{\partial N/N}\right)_{ss} \frac{\alpha_{Lss}\bar{T}_{ss}Y_{ss}A_{ss} + \alpha_{Lf}\bar{T}_f Y_f A_f}{\left(Y_{ss}A_{ss} + Y_f A_f\right)\beta} \left(1 - F_{\mathrm{LowBU}}\right)$$

The radial and axial weighting of the steel expansion reactivity is carried out in the same manner as for the fuel expansion reactivity. The radial steel reactivity worth shape factor is entered as XRSSHP (Input Block 62, location 270), and the axial shape is taken as the normalized axial shape of input array CLADRA (Input Block 62, location 160).

4.5.9.3.2 Radial Expansion

The reactivity feedback due to radial expansion of the cladding results from the displacement of sodium from the core. This removal is independent of the burnup because the expansion is directed toward the coolant channel. The expression for the radial expansion of the stainless steel structure is:

$$\zeta_{ssr} = -2\frac{V_{ss}}{V_{\mathrm{Na}}}\left(\frac{\partial k}{\partial N/N}\right)_{\mathrm{Na}}\frac{\alpha_{Lss}\bar{T}_{ss}}{\beta}$$

where V_{ss} is the volume of stainless steel in the cladding, and ζ_{ssr} is the reactivity feedback due to radial expansion of the clad.

The same type of summation as given above (Section 4.5.9.1.3) is used to volume weight the reactivities.

4.5.9.4 Axial Reflector Sodium Expansion

In the axial reflector the reactivity feedbacks stem mostly from the change in leakage. The upper and lower axial reflector sodium expansion are treated as linear effects.

4.5.9.4.1 Upper Reflector

The expression for the upper reflector sodium parameter ζ is:

$$\zeta_{ur} = \left(\frac{\partial k}{\partial T}\right)_{ar}\frac{\bar{T}_{ur}}{\beta}$$

where $\bar{T}_{ur}$ is the average temperature in the upper reflector, and $(\partial k/\partial T)_{ar}$ is the change in k with respect to a change in axial reflector temperature.

The input value for the above partial derivative is entered as variable YRCUR (Input Block 12, location 459).

To determine the average temperature of the coolant in the upper reflector, the following equation is used:

$$\bar{T}_{uf} = \frac{\sum_{i=1}^{N} V_i T_i + \sum_{j=1}^{M}\sum_{k=1}^{L(j)} V_{j,k} T_{j,k}}{\sum_{i=1}^{N} V_i + \sum_{j=1}^{M}\sum_{k=1}^{L(j)} V_{j,k}}$$

where N is the number of axial nodes in the gas plenum, M is the number of zones in the upper reflector, $L(j)$ is the number of axial nodes in zone j. Also, V_i is the volume of coolant node i in the plenum space, T_i is the temperature of the node i coolant in the

plenum space, $V_{j,k}$ is the volume of coolant node k in zone j in the reflector area, and $T_{j,k}$ is the temperature of the coolant in node k of zone j in the reflector area.

In this analysis, only the sodium coolant is considered to determine the reactivity feedback. This is done for two reasons: the difference between the sodium coolant and stainless steel temperature is small and the relative contributions of the stainless steel and coolant expansions are unknown. The volumes used are that of the flow, not of the structure and flow.

4.5.9.4.2 Lower Reflector

The expression for the lower reflector sodium feedback is:

$$\zeta_{lr} = \left(\frac{\partial k}{\partial T}\right)_{ar} \frac{\overline{T}_{lr}}{\beta}$$

where the partial derivative is entered as input variable YRCLR (Input Block 12, location 460) and $\overline{T}_{lr}$ is the average temperature in the lower reflector.

The same temperature volume-weighting scheme used in the upper reflector is also used in the lower reflector. Again, the temperatures are that of the coolant and the volumes are that in which flow occurs.

4.5.9.5 Radial Reflector Expansion

The reactivity change that results from a temperature change in the radial reflector is mainly due to the change in density of the sodium in the reflector, which results in a change in the leakage. The radial reflector expansion is treated as a linear effect. The expression for the radial reflector sodium feedback is:

$$\zeta_{rr} = \left(\frac{\partial k}{\partial T}\right)_{rr} \frac{\overline{T}_{rr}}{\beta}$$

where $(\delta k/\delta T)_{rr}$ is the change in k with respect to the radial reflector temperature, and $\overline{T}_{rr}$ is the average temperature of the radial reflector.

The partial derivative is entered as input variable YRCRR (Input Block 12, location 461). The nodes from which the average temperature is determined are those in which LCHTYP is set to 2, indicating a stainless steel reflector subassembly, and those of the bypass region at the core level. For the channel subassemblies, only zone 5 (currently the core) is used in the volume weighting. For the bypass channel, the temperatures are also volume weighted. The coolant temperature is volume weighted in all axial nodes of all channels to obtain the average temperature. The equation used in the code is:

$$\overline{T}_{rr} = \frac{\sum_i V_{by,i} T_{by,i} + \sum_j V_{ch,j} T_{ch,j}}{V_{by} + V_{ch}}$$

where $V_{by,i}$ is the volume of bypass region i, $T_{by,i}$ is the temperature of the bypass region i, V_{by} is the total volume of the bypass region corresponding to the reflector, $V_{ch,j}$

is the volume of axial layer j of the stainless steel containing channel, $T_{ch,j}$ is the temperature of axial layer j of the stainless steel containing channel, V_{ch} is the total volume of the stainless steel channel.

4.5.9.6 Doppler Effect

The Doppler effect is a nonlinear phenomenon that results from the change in effective cross sections at different temperatures. The temperature coefficient for the Doppler effect $(\delta k/\delta T)_D$ is a function of fuel temperature:

$$\left(\frac{\partial k}{\partial T}\right)_D = \frac{k_D}{\overline{T}_f}$$

where k_D is an input variable YRCDOP (input Block 12, location 464) and $\overline{T}_f$ is the channel average fuel temperature. Since the Doppler temperature coefficient is temperature dependent, an average value is used.

$$\left\langle\left(\frac{\partial k}{\partial T}\right)_D\right\rangle = \frac{\int_{\overline{T}_f(0)}^{\overline{T}_f(t)}\left(\frac{\partial k}{\partial \overline{T}}\right)_D d\overline{T}_f}{\int_{\overline{T}_f(0)}^{\overline{T}_f(t)} d\overline{T}_f} = \frac{k_D}{\overline{T}_f(t)-\overline{T}_f(0)}\ln\left[\frac{\overline{T}_f(t)}{\overline{T}_f(0)}\right]$$

where $\overline{T}_f(t)$ is the channel average fuel temperature at time t, and $\overline{T}_f(0)$ is the steady-state channel average fuel temperature.

The total feedback δk_D due to the Doppler effect is the sum of the Doppler feedbacks for each fueled channel. This is implemented in the code as:

$$\delta k_D = \sum_{i=1}^{N}\left\langle\left(\frac{\partial k}{\partial T}\right)_D\right\rangle_i \frac{V_i}{V_{\text{tot}}}\left[\overline{T}_{f,i}(t)-\overline{T}_{f,i}(0)\right] = \frac{k_D}{V_{\text{tot}}}\sum_{i=1}^{N} V_i \ln\left[\frac{\overline{T}_{f,i}(t)}{\overline{T}_{f,i}(0)}\right]$$

where the temperatures given above are currently weighted by the axial and radial reactivity worths.

4.5.9.7 Control Rod Bank Expansions

The change in reactivity that results from control rod bank temperature change is a result of the support of these rods. These are suspended from the top of the reactor. When a temperature change occurs, the rods expand or contract, forcing some of the fuel into or out of the core. This results in a reactivity change. The control rod expansion is treated as a linear effect. Although there are several portions of the control rod that undergo expansion when the temperature is increased, the current code only models two. The first of these is the control rod fuel and the second is the driveline expansion. The expression found in the code is:

$$\zeta_{cr} = \frac{\left(\frac{\partial k}{\partial T}\right)_{cr}}{\beta}\left[F_{cr}\frac{\sum_{i=1}^{N}\overline{T}_{f,i}V_i}{V_{\text{tot}}} + (1-F_{cr})T_{CV2}\right]$$

where T_{CV2} is the temperature in the upper plenum (CV#2 in SASSYS), $(\delta k/\delta T)_{cr}$ is the change is the change in k with respect to control rod temperature, and F_{cr} is the fraction of the response due to the channel temperature change.

The partial derivative above is entered as input variable YRCCR (Input Block 12, location 462) and F_{cr} is entered as FCR (Input Block 12, location 468).

The model given above differs from previous models [Ref. 4-12] because it does not include different time constants which characterize the different portions of the stainless steel control rod structure; instead, they are treated as the two terms given above; one proportional to fuel temperature and the other proportional to the exit plenum temperature. For steady state or a series of steady states this will not result in any significant error.

4.5.9.8 Upper Grid Plate Expansion

The upper grid plate is located below the core and serves as a support for the hex can. Grid plate expansion impacts the reactivity by displacing the assembly rows in the reactor. The upper grid plate expansion is treated as a linear effect. Reference 4-9 gives the following expression for the feedback:

$$\zeta_{gp} = \frac{T_{CV1}(t)}{\beta}\left(\frac{\partial k}{\partial T}\right)_{gp}$$

where ζ_{gp} is the reactivity due to the upper grid plate expansion, $T_{\mathrm{CV1}}(t)$ is the temperature of the inlet plenum (CV#1 in SASSYS), and $(\delta k/\delta T)_{gp}$ is the feedback coefficient associated with the grid plate.

The partial derivative above is an input parameter entered as YRCGP (Input Block 12, location 463).

4.5.9.9 Bowing and Unspecified Parameters

In the EBR-II reactivity feedback model, "bowing" is a "catch all" for terms which can not specifically be identified and therefore may contain terms other than that which result from the bowing of the assembly. True assembly bowing results when one side of a fuel assembly is at a higher temperature than the other. This results in a different expansion of the two sides moving the assembly radially. Bowing contributes to the reactivity by increasing or decreasing the amount of fuel in relatively high worth portions of the core.

The overall “bowing” term in the EBR-II model is treated as a linear effect that is modeled by one line below a threshold and by another line above the threshold. The effect is a function of the normalized temperature rise across the core ΔT_{norm}. For normalized temperatures above the threshold, which is given by the input variable YTCUT (Input Block 12, location 469), the bowing reactivity δk_{bw} is given by:

$$\delta k_{bw} = A + B\Delta T_{\mathrm{norm}}$$

For normalized temperatures below the threshold, the bowing reactivity δk_{bw} is given by:

$$\delta k_{bw} = \left(\frac{A}{\text{YTCUT}} + B\right) \Delta T_{\text{norm}}$$

The values for the input coefficients A and B are entered as YABOW and YBBOW (Input Block 12, location 466 and 467).

The normalized temperature rise is the ratio of the temperature rise across the core at time t to the temperature rise across the core at full power and flow conditions. The temperature rise is modeled as the difference between the upper and lower plena temperatures (found in YTLCV2 and YTLCV1) or as the difference between the average sodium temperature for the fueled channels $\bar{T}_{\text{Na}}$ and the temperature of the lower plenum YTLCV1. Which model is used for the normalized temperature rise is determined by an input parameter IBOWTP (Input Block 1, location 102). For IBOWTP equal to zero, the normalized temperature rise is based on the outlet and inlet plena temperatures. In the case, the normalized factor YDELT0 (Input Block 12, location 465) gives the difference between the outlet and inlet plena temperatures at full power and flow conditions. For IBOWTP not equal to zero, the normalized temperature rise is based on the average sodium temperature in fueled channels and the temperature of the inlet plenum. In this case, the normalized factor YDELT0 gives the difference between the average sodium temperature in the fueled channels and the temperature of the inlet plenum at full power and flow conditions.

4.6 Solution Methods

The SAS4A/SASSYS-1 point kinetics equations are solved using a technique model by Kaganove [4-13] and extended by Fuller [4-14]. The decay-heat model is solved according to the method developed by Woodruff for the SAS3A computer code [4-1]. In general, the SAS4A/SASSYS-1 neutronics solution methods have been adopted from SAS3A.

4.6.1 Point Kinetics

The solution of the point kinetics model equations is carried out assuming that (1) the reactivity has been specified, and (2) the number of delayed-neutron precursors is limited to six or less. This latter assumption requires the interpretation of the precursor yields and decay constants as average values, typical for a particular blend of isotopes.

Given these assumptions, the first step in the solution of the point kinetics equations is the integration of the delayed-neutron precursor energy production balance equations given by Eq. 4.3-1 over a time interval. In SAS4A/SASSYS-1, this time interval is taken as the main time step. If conditions are known at time t, then integration of Eq. 4.3-1 to time $t + \Delta t$ gives

$$C_i(t+\Delta t) = C_i(t)e^{-\lambda_i \Delta t} + \frac{\beta_i}{\Lambda} e^{-\lambda_i (t+\Delta t)} \int_t^{t+\Delta t} \phi(t') e^{-\lambda_i t'} dt' \qquad (4.6\text{-}1)$$

The expressions given by Eq. 4.6-1 for the C_i at the advanced time are substituted directly into Eq. 4.2-4. Next, the time variation of the fission power amplitude over the time step is assumed to be

$$\phi(t+\Delta t) = \phi(t) + \phi_1 \Delta t + \phi_2 (\Delta t)^2 \qquad (4.6\text{-}2)$$

where ϕ_1 and ϕ_2 are constants to be determined. To find ϕ_1 and ϕ_2, Eq. 4.6-2 is first differentiated and substituted for in Eq. 4.2-4. In addition, Eq. 4.6-2 is substituted directly for in Eqs. 4.2-4 and 4.6-1. The integral term in Eq. 4.6-1 is evaluated analytically. This yields a single equation in the two unknowns ϕ_1 and ϕ_2. To obtain ϕ_1 and ϕ_2, this equation is evaluated for the full time step Δt, and for the half time step $\Delta t/2$, to give two linear equations in the two unknowns. Solution of this equation set yields ϕ_1 and ϕ_2, and thus an estimate of $\phi(t+\Delta t)$.

To control the precision of this approximate solution method, an internal time-step control algorithm has been implemented. In addition to the full time-step solution, a half time step solution is also obtained (i.e. evaluation of Eq. 4.2-4 at Δt/2 and Δt/4). The half-step solution is extrapolated to the end of the time step and compared with the full step solution. If the fractional difference is within a user-specified tolerance, the full-step solution is accepted. If not, the internal time step is halved and the entire solution process is repeated. This procedure is carried out until the solution is advanced to the end of the main time step. The half/full-step fission power amplitude convergence precision is entered as EPSPOW (Input Block 11, location 3).

On each main time step, the point kinetics solution is obtained twice. At the beginning of the time step, the net reactivity is linearly extrapolated in time to the end of the time step, and a solution for ϕ is obtained with this extrapolated value. This solution is then used to drive the energy equation solutions in the SAS4A/SASSYS-1 models through the time step. When all channels have been advanced to the end of the main time step, the reactivities are calculated and the net reactivity is used to solve once more for ϕ. This second solution is taken as the final value for the time step, and solutions for the delayed-neutron precursor and decay-heat equations are based on this value.

For long, slow transients, an oscillation or instability in the solution for reactivity and power has been observed when time steps larger than 0.25 seconds are used. Modifications to the code have been made to eliminate this instability or oscillation. With the modified code, time step sizes of 1 second can be used in the early part of the transient, when flows and temperatures are changing rapidly, and 5 second step sizes can be used after the first few hundred seconds of the transient. The oscillations or instabilities come about because the reactivity used to compute the power level for a time step is an extrapolated reactivity, based on the last two previous computed steps. The extrapolated reactivity is used to compute a power level that is then used to

compute fuel pin temperatures. After the temperatures are computed, the reactivity is computed. The computed reactivity may not be the same as the extrapolated reactivity. If the extrapolated reactivity is high, it will lead to higher fuel temperatures, which will lead to a lower computed reactivity. For the next step the extrapolated reactivity will be low, and the computed reactivity will be high. For large time steps, this leads to oscillations. The fuel expansion and Doppler reactivity oscillate up-down-up-down from step to step.

Adding a correction term to the extrapolated reactivity, k_{ext}^{n}, for time step n eliminated the oscillations. First an error, e_n, is calculated as the difference between the computed reactivity, k^n, and the extrapolated reactivity:

$$e_n = k^n - k_{\text{ext}}^{n} \tag{4.6-2a}$$

Then the reactivity k' actually used for step n is computed as

$$k' = k_{\text{ext}}^{n} + |e_{n-1}|\text{sign}(e_{n-2}) \tag{4.6-2b}$$

The correction term tends to cancel out the oscillations. The application of this correction is controlled by input variable JREEXT (Input Block 1, location 56).

4.6.2 Decay Heat

Given the known time dependence of the fission-power amplitude, the equation for the normalized decay heat energy production, Eq. 4.4-1, may be integrated directly to obtain the advanced time value. As implemented, a maximum of six decay-heat groups is allowed, so that the decay constants and yields are taken to be averaged quantities. Integration of Eq. 4.4-1 yields

$$h_{nk}(t+\Delta t) = h_{nk}(t)e^{-\lambda_{hnk}\Delta t} + \beta_{hnk}e^{-\lambda_{hnk}(t+\Delta t)}\int_{t}^{t+\Delta t}\phi(t')e^{\lambda_{hnk}t'}dt' \tag{4.6-3}$$

where the time step, Δt, is taken as the internal point kinetics time step and the functional dependence of the fission power amplitude is given by Eq. 4.6-2 with the known values of ϕ_1 and ϕ_2. The integral term in Eq. 4.6-3 is evaluated analytically.

In the evaluation of the integral in Eq. 4.6-3, the following types of expressions occur:

$$I_{1nk} = 1 - e^{\lambda_{hnk}\Delta t} \tag{4.6-4a}$$

$$I_{2nk} = \lambda_{hnk}\Delta t - I_{1nk} \tag{4.6-4b}$$

$$I_{3nk} = (\lambda_{hnk}\Delta t)^2 - 2I_{2nk} \tag{4.6-4c}$$

Evaluation of Eqs. 4.6-4 in the order listed for small time steps ($\lambda_{hnk}\Delta t < 0.01$) results in unacceptable propagation of small, numerical round-off errors in the calculation of the exponential in I_{1nk}. Therefore, for small time steps, a series expansion of the exponential term is used along with an inverted recursion order as

$$I_{3nk} = 2\frac{(\lambda_{hnk}\Delta t)^3}{3!} - \frac{(\lambda_{hnk}\Delta t)^4}{4!} + \frac{(\lambda_{hnk}\Delta t)^5}{5!} - \cdots \tag{4.6-5a}$$

$$I_{2nk} = \frac{1}{2}[(\lambda_{hnk}\Delta t)^2 - I_{3nk}] \tag{4.6-5b}$$

$$I_{1nk} = \lambda_{hnk}\Delta t - I_{2nk} \tag{4.6-5c}$$

4.6.3 Specified Power History

The point kinetics and decay-heat models may be overridden through the specification on input of a user-supplied power history. This option is intended to be used for analyses in which the power history is known, such as those for in-pile experiments. It is also possible to specify an external, driving reactivity that is summed with the internally calculated feedback reactivity. This option may employ either a user-specified subroutine function named PREA, or a user-specified table of input power (or reactivity) values for input problem time values. The choice of specifying power or external reactivity is controlled with input variable IPOWER (Input Block 1, location 8), and the choice of an input function or table is set by NPREAT (Input Block 1, location 18), which gives the number of entries in the power (or reactivity) table and defaults to zero, which indicates usage of the input function PREA. Should a PREA not be supplied for this case, steady-state power or reactivity conditions are assumed.

For NPREAT > 0, input values for the power (or reactivity) and problem times at which they apply are entered in arrays PREATB and PREATM (Input Block 12, locations 29 - 48 and 49 - 68).

When the power vs. time option is invoked (IPOWER = 1), additional power tables may be entered by setting NPOWDK (Input Block 1, location 45) to the total number of tables to be input (2, …, 5), and entering the additional power vs. time table in arrays PRETB2 and PRETM2 (Input Block 12, locations 100–179 and 180–259). (The first table is always entered in PREATB and PREATM). Input integer IDKCRV (Input Block 51, location 203) then specifies the input power curve to be used in a particular channel. Note that this multiple input power table option is only available for IPOWER = 1 and NPOWDK > 1.

4.7 Code Organization and Data Flow

The subroutines in SAS4A/SASSYS-1 that are mainly related to the solution of the reactor kinetics, decay-heat, and reactivity feedback models are listed in Table 4.7-1. Most of these routines are called directly from the steady-state and transient driver routines, SSTHRM and TSTHRM. Flow diagrams for these routines are included in Section 2.2.

Table 4.7-1. Listing of Reactor Kinetics Subroutines

Subroutine	Description
SSPK	Initializes all steady-state point kinetics data including power, reactivity, delayed-neutron precursor concentrations, and decay heat sources.
POWINT	Extrapolates power at the beginning of a main time step for external power vs. time option via call to PREA. Updates parabolic power history coefficients.
PREA	User-supplied external power or reactivity history.
PAR	Fits a parabola to three points.
POINEX	Extrapolates reactivity at the beginning of a main time step for reactivity vs. time option by parabolic extrapolation of calculated internal reactivity and direct evaluation of external reactivity via call to PREA.
TSPK	Given an extrapolated or calculated reactivity, drives the calculation of the reactor power. Resets beginning time-step values and calls PKSTEP.
PKSTEP	Performs the integration of the point kinetics equations across a main time step.
RHOEND	Updates end-of-time step values.
FEEDBK	Performs calculation of Doppler and coolant void reactivity feedback for a channel.

At steady state, the driver routine SSTHRM calls subroutine SSPK, which performs all required data initialization. In the transient calculation, the point kinetics equations are solved on each main time step. From driver routine TSTHRM, subroutine POWINT is called at the beginning of each main time step to provide an extrapolation in time of the reactor power for the power versus time option (IPOWER = 1). For the reactivity versus time option (IPOWER = 0), subroutine POINEX is called to provide an extrapolation of the reactivity, and subroutine TSPK is then called to compute the reactor power given the reactivity. Subroutine TSPK performs data initialization and calls subroutine PKSTEP, which integrates the point kinetics and decay-heat equations over the main time step. At the end of the main time step, subroutine FEEDBK is called from driver routine TSTHRM to compute the current reactivity feedback, and subroutine TSPK is called once more to compute the final estimate of the reactor power. Subroutine

RHOEND is then called to update the coefficients used in the integration of the point kinetics equations.

4.8 Input/Output Description

Table 4.8-1 contains a listing of SAS4A/SASSYS-1 input locations that are relevant to the point kinetics, reactivity feedback, and decay-heat models. A complete SAS4A/SASSYS-1 input description may be found in Appendix 2.2.

On each main time step, the following quantities are printed: a) total reactor power (normalized to unity at time zero), b) decay-heat power, c) integrated energy (full-power seconds), d) net reactivity, e) programmed reactivity, f) control rod drive expansion reactivity, g) Doppler reactivity, h) fuel and cladding axial expansion reactivity, i) coolant reactivity, j) fuel-motion reactivity, and k) cladding-motion reactivity. In addition, the coolant, fuel, cladding, axial expansion and Doppler reactivity for each channel are also printed at each main time step. This information is also printed following each major print in expanded form (more significant digits), along with the group-wise values of the delayed-neutron precursor concentrations and decay-heat powers.

Table 4.8-1. Point Kinetics, Decay-Heat, and Reactivity Feedback Input Data

Symbol	Reference	Name	Block	Location	Suggested Value
–	–	IPOWER	1	8	0 or 1
–	Appendix 4.1	IPOWOP	1	9	0 or 1
–	–	NPK	1	10	0
–	–	NDELAY	1	16	≥0, ≤6
–	–	NDKGRP	1	17	≥0, ≤6
–	–	NPREAT	1	18	≥0, ≤20
–	–	ICREXP	1	31	≥0, ≤3
–	–	IDBPWI	1	35	0 or 1
–	–	IRADEX	1	36	≥−7, ≤7
–	–	NFUELD	1	39	<0
–	–	NOREAC	1	41	≥0
–	–	NSRMTB	1	43	Not used.
–	–	NPOWDK	1	45	≥0,≤5
–	–	NPDKST	1	46	≥0,≤8
–	–	NSUBTC	1	51	≥0
–	–	MTGRD	1	52	1 or 2
–	–	MTACLP	1	53	1 or 2
–	–	MTTLP	1	54	1 or 2

Symbol	Reference	Name	Block	Location	Suggested Value
–	–	MODEEX	1	55	≥0, ≤3
–	–	JREEXT	1	56	0 or 1
–	–	IREACT	1	58	≥−2, ≤2
–	–	NSUBTR	1	59	≥0
–	–	NRRNGS	1	60	0,1, or 2
–	–	MTRRAC	1	61	1 or 2
–	–	MTRFAC	1	63	1 or 2
–	–	MTRFT	1	64	1 or 2
–	–	IROPT	1	65	0 or 1
–	–	JCRIND	1	66	>0
–	–	ICRDDB	1	71	0,1, or 2
–	–	ICRTMP	1	72–74	≥0
–	–	ICRNOD	1	75–77	–
–	–	NSEGCR	1	78	>0
–	–	MTCB	1	81	1 or 2
–	–	KDEBUG	1	82	0 or 1
–	–	KEBRS1	1	83	≥0
–	–	KEBRS2	1	84	≥0
–	–	IDBDKH	1	85	–
–	–	NULLD3	1	86	–
–	–	NOFDBK	1	89	≥0
–	–	IBOWTP	1	102	0 or 1
–	–	KCHUIS	3	1209–1242	Not used.
–	–	NRREAC	3	1292	≥0
–	–	ISLREA	3	1293–1300	≥0
–	–	LBYP	3	1301	≥0
–	–	LELBYP	3	1302–1309	≥0
–	–	EPSPOW	11	3	10^{-4}
–	–	ASCRAM	11	23	Not used.
–	–	PSCRAM	11	24	Not used.
–	–	GSCRAM	11	25	Not used.
–	Appendix 4.1	POW	12	1	–
Λ	(4.2-4)	GENTIM	12	2	–

Symbol	Reference	Name	Block	Location	Suggested Value
–	Appendix 4.1	POWTOT	12	3	–
β_i	(4.3-1)	BETADN	12	4–9	–
λ_i	(4.3-1)	DECCON	12	10–15	–
–	–	OLDBDK	12	16–21	Not used.
–	–	OLDDKL	12	22–27	Not used.
–	–	OLDBDT	12	28	Not used.
–	–	PREATB	12	29	–
–	–	PREATM	12	49	–
–	Appendix 4.1	FRPR	12	69	–
L_{cr}	(4.5-36)	CRDLEN	12	71	–
α_{cr}	(4.5-36)	CRDEXP	12	72	–
a_{cr}	(4.5-39)	ACRDEX	12	73	–
b_{cr}	(4.5-39)	BCRDEX	12	74	–
$M_{cr}C_{cr}$	(4.5-29)	CRDMC	12	75	–
$h_{cr}A_{cr}$	(4.5-29)	CRDHA	12	76	–
V_{ui}	(4.5-30)	UIVOL	12	77	–
C_{rc}	(4.5-23)	RDEXPC	12	78	–
XMC/XAC	(4.5-23)	XMCXAC	12	79	–
–	–	SCRTAB	12	80	Not used.
–	–	SCRTME	12	90	Not used.
–	–	PRETB2	12	100–179	–
–	–	PRETM2	12	180–259	–
β_{hnk}	(4.4-1)	BETADK	12	260–289	–
λ_{hnk}	(4.4-1)	DKLAM	12	290–319	–
β_{hk}	–	BETAHT	12	320–324	–
P_i	(4.4-3)	POWLVL	12	325–364	–
t'	(4.4-3)	POWTIM	12	365–404	–
S_{GRMAX}	(4.5-27)	SLMAX	12	408	–
–	–	PITCHG	12	409	–
–	–	PITCHA	12	410	–
–	–	PITCHT	12	411	–
–	–	RDEXCF	12	412	–
–	–	TLPRRC	12	413	–
–	–	BNDMM1	12	414	–

Symbol	Reference	Name	Block	Location	Suggested Value
–	–	BNDMM2	12	415	–
–	–	TINSRT	12	416	–
–	–	REAINS	12	417	–
–	–	TLIMIT	12	418	–
–	–	DFLTCS	12	419	–
–	–	DFLTSS	12	420	–
–	–	ACLPRC	12	421	–
–	–	FCDTR1	12	422	–
–	–	FCDTR2	12	423	–
–	–	FCDTRF	12	424	–
–	–	DRCOLL	12	425	–
–	–	CRSAC	12	426	–
–	–	RR1TC	12	427	–
–	–	RR2TC	12	428	–
–	–	RODID	12	429	–
–	–	RODOD	12	430	–
–	–	SHRDLN	12	431–433	–
–	–	SHRDID	12	434–436	–
–	–	SHRDOD	12	437–439	–
–	–	RHOCRD	12	440	–
–	–	HTCPCR	12	441	–
–	–	CONDCR	12	442	–
–	–	VFCRD	12	443	–
–	–	HFILM	12	444	–
–	–	FLSHRD	12	445	–
–	–	AREACR	12	446	–
–	–	FLOEXP	12	447	–
–	–	ACLPEL	12	448	–
–	–	TLPEL	12	449	–
–	–	PTCHRA	12	450	–
–	–	PTCHRT	12	451	–
–	–	RCBARR	12	452	–
–	–	FCDTCB	12	453	–
–	–	CB2TC	12	454	–

Symbol	Reference	Name	Block	Location	Suggested Value
–	–	YKNF	12	455	–
–	–	YKHF	12	456	–
–	–	YKNNA	12	457	–
–	–	YKNSS	12	458	–
–	–	YRCUR	12	459	–
–	–	YRCLR	12	460	–
–	–	YRCRR	12	461	–
–	–	YRCCR	12	462	–
–	–	YRCGP	12	463	–
–	–	YRCDOP	12	464	–
–	–	YDELT0	12	465	–
–	–	YABOW	12	466	–
–	–	YBBOW	12	467	–
–	–	FCR	12	468	–
–	–	YTCUT	12	469	–
ε_{ex}	–	EXPCOF	13	1263	–
–	–	IAXEXP	51	181	0, 1, or 2
–	–	IDKCRV	51	203	≥0, ≤5
–	–	ICHUIS	51	362	0 or 1
–	–	IPOWRZ	51	364	0 or 1
–	–	IREACZ	51	365	0 or 1
γ_s	3.3-22	GAMSS	62	2	–
γ_c	3.3-22	GAMTNC	62	4	–
γ_e	3.3-22	GAMTNE	62	5	–
$\bar{P}$	Appendix 4.1	PSHAPE	62	6–29	–
P_r	–	PSHAPR	62	30–44	–
α_D	(4.5-2)	ADOP	62	62	–
α_D	(4.5-2)	BDOP	62	63	–
–	–	WDOPA	62	64–111	–
$(\rho_c)_{jI}$	(4.5-22)	VOIDRA	62	112–159	–
R_e	–	CLADRA	62	160–207	–
R_f	(4.5-20)	FUELRA	62	208–255	–
–	Appendix 4.1	PRSHAP	62	256	–

Symbol	Reference	Name	Block	Location	Suggested Value
–	–	PSHPTP	62	257–261	–
–	–	PSHPBT	62	262–266	–
–	–	XRFSHP	62	268	–
–	–	XRNSHP	62	269	–
–	–	XRSSHP	62	270	–
–	–	PSHAPC	62	271–318	–
–	–	PSHAPB	62	319–366	–
α_f	(4.5-4)	FUELEX	63	73	–
α_e	(4.5-5)	CLADEX	63	74	–
Y_f	(4.5-8)	YFUEL	63	75	–
Y_e	(4.5-8)	YCLAD	63	76	–
ε_{ex}	(4.5-21)	EXPCFF	63	79	–

REFERENCES

NOTICE

Several references in this document refer to unpublished information. For a list of available open-literature citations, please contact the authors.

APPENDIX 4.1:
STEADY-STATE POWER NORMALIZATION IN SAS4A/SASSYS-1

The power in axial fuel pin segment I of channel J is given by the expression

$$\text{PSHAPE}(I,J) \times \text{QMULT} \times \text{POW}$$

Here POW is the maximum power of any axial fuel pin segment. QMULT is a multiplier that is equal to one in steady state.

PSHAPE(I,J) is the ratio of the power of segment (I,J) to the maximum power of any segment. It is obvious that PSHAPE takes values between zero and one.

SAS4A/SASSYS-1 will renormalize the input values of PSHAPE and PRSHAP. This is done is subroutine PNORM. The user needs only supply un-normalized data for these arrays.

PNORM will also compute POW from POWTOT or POWTOT from POW according to the value of IPOWOP.

Input:

IPOWOP = 0	Calculate steady-state power in peak axial segment from total reactor power.
IPOWOP = 1	Calculate steady-state total reactor power from the peak axial fuel pin segment.
POWTOT	Total reactor power in steady state.
POW	Steady-state power in the peak axial pin segment.
FRPR	Fraction of total reactor power represented by sum of all SAS4A/SASSYS-1 channels.
NPIN(ICH)	Number of fuel pins in a subassembly of channel ICH.
NSUBAS(ICH)	Number of subassemblies in channel ICH.
MZ(ICH)	Number of axial nodes in channel ICH.
PRSHAP(ICH)	The relative power per subassembly in channel ICH. PRSHAP will be normalized by PNORM.
PSHAPE(I,ICH)	The relative power per axial pin segment of axial pin segment I and channel ICH. I = 1, … MZ(ICH). PSHAPE will be normalized by the PNORM routine.

Method:

The values of PRSHAP get renormalized as RELCHA for all channels:

$$\text{RELCHA}(ICH) = \text{PRSHAP}(ICH) \times \frac{\sum_I \text{NSUBAS}(I)}{\sum_I \text{PRSHAP}(I) \times \text{NSUBAS}(I)}$$

If we multiply the above equation by $\text{NSUBAS}(ICH)$ and then sum over all channels ICH, we can show that

$$\sum_{ICH} \text{RELCHA}(ICH) \times \text{NSUBAS}(ICH) = \sum_{ICH} \text{NSUBAS}(ICH)$$

Thus, RELCHA is properly normalized.

The values of PSHAPE get normalized as RELSHP for each channel:

$$\text{RELSHP}(IZ, ICH) = \frac{\text{PSHAPE}(IZ, ICH)}{\sum_I \text{PSHAPE}(I, ICH)}$$

If we sum over all axial nodes IZ, we can show that

$$\sum_{IZ} \text{RELSHP}(IZ, ICH) = 1$$

Thus, RELSHP is properly normalized.

The power of axial pin segment (I, J) is

$$\text{RELSHP}(I, J) \times \frac{\text{RELCHA}(J)}{\text{NPIN}(J)} \times \frac{\text{FRPR} \times \text{POWTOT}}{\sum_{ICH} \text{NSUBAS}(ICH)}$$

From the definition of POW we get the equation

$$\text{POW} = \max_{I,J} \left[\text{RELSHP}(I, J) \times \frac{\text{RELCHA}(J)}{\text{NPIN}(J)} \right] \times \frac{\text{FRPR} \times \text{POWTOT}}{\sum_{ICH} \text{NSUBAS}(ICH)}$$

and the unknown POWTOT or POW can be found. Given $I_{\max}$ and $J_{\max}$ to be the indices of the peak power pin segment, we then redefine $\text{PSHAPE}(I, J)$ as

$$\text{PSHAPE}(I, J) = \frac{\text{RELSHP}(I, J) \times \text{RELCHA}(J)}{\text{NPIN}(J)} \times \frac{\text{NPIN}(J_{\max})}{\text{RELSHP}(I_{\max}, J_{\max}) \times \text{RELCHA}(J_{\max})}$$

This is the desired form of PSHAPE that is used by the subroutine SHAPE.